INVESTIGATION OF OIL FLOW AND HEAT TRANSFER IN TRANSFORMER RADIATOR

A Thesis Submitted to
The Graduate School of Engineering and Sciences of
Izmir Institute of Technology
In Partial Fulfillment of the Requirements for the Degree of

MASTER OF SCIENCE

in Energy Engineering

by
Özben KAYMAZ

December 2015
İZMİR

We approve the thesis of **Özben KAYMAZ**

Examining Committee Members:

_____

Assoc. Prof. Dr. Tahsin BAŞARAN
Department of Architecture, Izmir Institute of Technology

_____

Prof. Dr. Gülden GÖKÇEN AKKURT
Department of Mechanical Engineering, Izmir Institute of Technology

_____

Assist. Prof. Dr. Mehmet Akif EZAN
Department of Mechanical Engineering, Dokuz Eylul University

23 December 2015

_____

Assoc. Prof. Dr. Tahsin BAŞARAN
Supervisor, Department of Architecure,
Izmir Institute of Technology

_____

Prof. Dr. Aytunç EREK
Co-Supervisor, Mechanical Engineering
Dokuz Eylul University

_____

Prof. Dr. Gülden GÖKÇEN AKKURT
Head of the Department of Energy
Engineering

_____

Prof. Dr. Bilge KARAÇALI
Dean of the Graduate School of
Engineering and Sciences

ACKNOWLEDGEMENTS

This study would not have been possible without the support of my family, professors and mentors, Balikesir Electromechanical Industrial Plants Co. (BEST Co.), my colleagues, and my friends.

I express my warmest gratitude to my family for encourage me in all of my pursuit and inspiring me to follow my dreams. I am especially grateful to my family, who helped me very much, especially when I was working in Balikesir and studying in Izmir.

I would like to express my deep gratitude to Energy Engineering Department of Izmir Institute of Technology professors and my advisor Assoc. Prof. Dr. Tahsin BAŞARAN for their invaluable advice and encouragement throughout the research. I would like to give my special thanks to my advisor for his endless supporting, leading, patience and motivation who always guided me during my higher education. He was always energetic and enthusiastic. He gave me the freedom I needed to move on and moral support when I was writing this thesis. I also thank my co-advisor Prof. Dr. Aytunç EREK from Mechanical Engineering Department of Dokuz Eylul University for his grateful advice and smartness.

I would very much like to BEST Co. and R&D Center for giving me this opportunity, continual supports and encouragement during this study. I would also like to extend my deepest gratitude to Dr. Gökhan KALKAN, who is the R&D Manager of BEST Co. for his kind help, endless effort to teach all his knowledge, generous advice and supporting me on my way to realize my dreams and my higher education. He was always solution oriented, whenever something went wrong or disappointing occurred. Special thanks to my workmates and friends, not only for understanding and supporting, but also for sincere friendship.

To all the people that I have met, thank you for sharing life with me and also for your friendship. I have a motto; ‘Share Knowledge!’. Because this thesis would not have been possible without sharing.

ABSTRACT

INVESTIGATION OF TRANSFORMER OIL FLOW AND HEAT TRANSFER IN TRANSFORMER RADIATOR

Transformer losses are produced by the current passing through resistance on the winding conductors. These losses are converted to heat energy as all electrical machines. Transformer life depends on the aging of cellulose-based insulation material in winding. Winding temperature must be kept below a certain temperature limit, because the excess heat in the windings directly accelerates the aging of insulation material. Oil-immersed transformers are cooled by using transformer oil. In this study, flow and heat transfer of transformer radiator filled with mineral oil, silicone oil and ester oil were investigated. Oil in radiator was modelled in 3D, thereby oil flow volume was created, heat transfer calculations were made with using different type transformer oils and investigation of flow behavior is studied. Temperature dependent density, thermal conductivity and viscosity values are obtained from oil suppliers. Transformer oil database was composed by using curve fitting methods in MathCAD Software to use in CFD (Computational Fluid Dynamics) analysis in Fluent software. Finally, the pressure differences were obtained for each oil type. According to the velocity versus pressure difference graph that was obtained from the results of this study, inertial resistance and viscous resistance could be described which are required in future studies to use porous medium approach. Number of elements and computation domain will be decreased by using porous medium approach, then complete transformer model could be analyzed. Additionally, thermal characteristics of transformer oils were obtained and compared in this study. Accordingly, natural ester oil had the best heat transfer and pressure drop.

ÖZET

TRANSFORMATÖR RADYATÖRÜNDE YAĞ AKIŞININ VE ISI TRANSFERİNİN İNCELENMESİ

Transformatör kayıpları sargı iletkeni üzerinden geçen direncin oluşturduğu akımdan kaynaklanır. Tüm elektrik makinelerinde olduğu gibi, oluşan kayıplar ısı enerjisine dönüşür. Transformatör ömrü, sargıda bulunan selüloz bazlı izolasyon malzemesinin yaşlanmasına bağlıdır. Sargı içerisinde oluşan fazla ısı doğrudan doğruya izolasyon malzemesinin yaşlanmasını hızlandırdığı için, sargı sıcaklığı önceden belirlenmiş olan sıcaklık sınırlarında tutulur. Yağlı tip transformatörler, transformatör yağı kullanılarak soğutulmaktadır. Bu çalışmada, mineral yağ, silikon yağ ve ester yağ kullanılan transformatör radyatöründe akış ve ısı transferi incelenmiştir. Radyatör içerisinde bulunan transformatör yağı 3 boyutlu olarak modellenmiş, böylece yağ akış hacmi oluşturulmuş, farklı tipte transformatör yağlarının ısı transferi hesaplamaları yapılmış ve akışın gösterdiği davranış incelenmiştir. Yağ tedarikçilerinden sıcaklığa bağlı olarak değişen yoğunluk, ısı sığası, ısıl iletkenlik ve viskozite değerleri sağlanmıştır. Transformatör yağına ait veriler, ANSYS Fluent simulasyon yazılımında HAD (Hesaplamalı Akışkanlar Dinamiği) analizlerinde kullanılmak üzere, MathCAD yazılımında eğri uydurma yöntemleri ile oluşturulmuştur. Sonuç olarak, rher bir yağ için radyatör boyunca oluşan basınç farkları elde edilmiştir. Bu çalışma neticesinde gelecek çalışmalarda gözenekli ortam yaklaşımının kullanılabilmesi amacı ile hıza bağlı olarak değişen basınç farkları grafiği elde edilmiştir. Böylece gözenekli ortam modellemesinde gerekli olan atalet direnci ve viskoz direnç katsayıları tanımlanabilecektir. Gözenekli ortam yaklaşımı kullanılarak, eleman sayısı ve çözüm süresi düşürülecek, böylece tüm bir transformatör analizi yapılabilecektir. Ayrıca, bu çalışma ile transformatör yağlarının karakteristikleri de elde edilerek, birbirleriyle karşılaştırılmıştır. Buna göre, doğal ester yağ, ısı transferi ve basınç düşümü açısından diğer yağlara göre daha iyi bir performans göstermiştir.

TABLE OF CONTENTS

LIST OF FIGURES

Figure **Page**

LIST OF TABLES

LIST OF SYMBOLS

Abbreviations

A	Area [m^2]
c	Specific thermal capacity [J/kg.K]
D_h	Hydraulic diameter [m]
g	Gravitational acceleration [m/s^2]
k	Thermal conductivity [W/m.K]
I_1	Current flowing through primary terminal [Ampere]
I_2	Current flowing through secondary terminal [Ampere]
T	Temperature [˚C or K]
T_0	Reference temperature [˚C or K]
h	Height [meter]
T_{inlet}	Inlet temperature [˚C or K]
L	Length [meter]
l	Length [meter]
N_1	Number of turns of the primary winding [-]
N_2	Number of turns of the secondary winding [-]
S	Distance [meter]
P	Pressure [Pascal]
P_{total}	Total cooling capacity of a radiator [Watt]
P_{fin}	Cooling capacity of a fin [Watt]
Q	Heat transfer [Watt]
Q_{oil}	Oil flow rate [m^3/s]
R	Resistance [Ohm]
t	Time [Second]
u	Vector along x axis [-]
V_1	Voltage drop at the primary terminal [-]
V_2	Voltage drop at the secondary terminal [-]
v	Vector along y axis [-]
w	Vector along z axis [-]

Greek Letters

ρ	Density [kg/m^3]
ρ_e	Electrical resistivity [ohm·meter]
μ	Dynamic viscosity [kg/m.s]
β	Thermal expansion coefficient [-]
α	Slope of the temperature rise [-]
ρ_0	Density of oil at the reference temperature [kg/m^3]
τ_{wall}	Wall shear stress [Pascal]

CHAPTER 1

INTRODUCTION

All the photos that have not any reference were used with the permission of Balikesir Electromechanical Industrial Plants Co.

Energy is directly related with the quality of human lives. The world-wide energy consumption is hugely increasing. In addition, dramatic increase in demand for oil is seen in recent years.

Electricity is generated in power plants from hydrothermal, natural gas, wind energy, solar energy and fossil fuel. These power sources rotate large turbines which are connected to generators at their other ends. Generated electricity in the generators is either 50 Hz. or 60 Hz. The maximum voltage level of the generated electricity is 20 kV. At this voltage level in order to transmit the electricity from the source to the end consumer large cable cross-sectional areas are required. This is definitely an expensive solution as the conductors using transmission lines are copper or aluminum. Moreover, DC losses in other loss I^2R losses are proportional to cross-sectional area of the used conductor. Therefore, at low voltage levels the losses occurred in the long transmission line generates excessive losses and the efficiency is reduced dramatically. As the resistance is formulated as,

$$R = \rho_e \frac{l}{A} \tag{1.1}$$

where, ρ_e is electrical resistivity, l is the length of the transmission line and A is the cross-sectional area of the current carrying conductor, the only solution to reduce the total cost of the transmission line is to decrease the cross-sectional area of conductor.

Volt/turns of the transformer at the primary and the secondary terminals has to be equal. This is formulated as,

$$\frac{V_1}{N_1} = \frac{V_2}{N_2} \tag{1.2}$$

where, V_1 is the voltage drop at the primary terminal, V_2 is the voltage drop at the secondary terminal, N_1 and N_2 are the number of turns of the primary and secondary windings, respectively.

Another important equation of transformers relates current of the terminals to the number of turns. This is formulated as,

$$N_1 I_1 = N_2 I_2 \tag{1.3}$$

where, I_1 and I_2 are the currents flowing through primary and secondary terminals, respectively.

From Equations (1.2) and (1.3), it can be seen that increasing the voltage at the terminal reduces the current. In other words, current and voltage are inversely proportional. This means that increasing the voltage level will generate substantial amount of decrease in the line current. Therefore, the losses occurs on the transmission line can be reduced.

Electrical energy is transmitted from power plants to electrical substations. Electricity is more efficiently transmitted at high voltages. Power transformers transmit the electricity at high voltages into substations. Distribution transformers convert the electricity to lower voltages. Electricity transmission steps were visualized by Southern Nevada Regional Professional Development Program as shown in Figure 1.

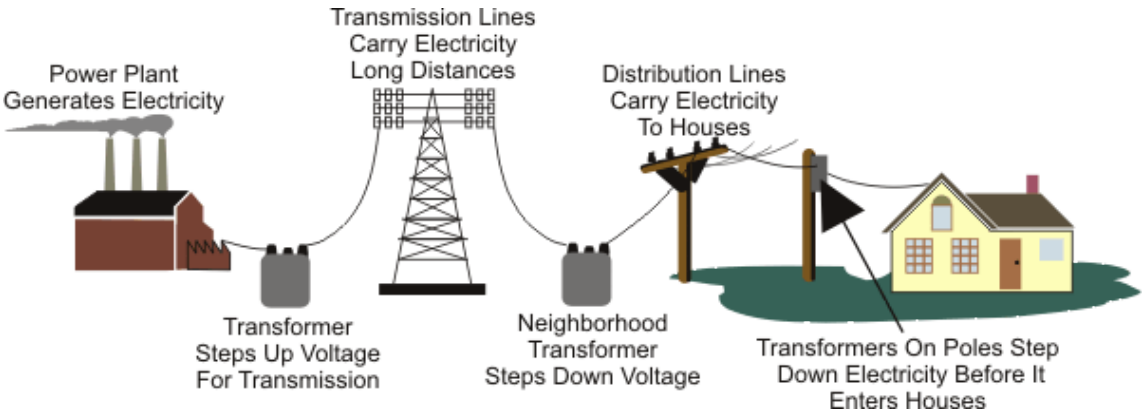

Figure 1. Electrical Transmission.

(Source: Retrieved October 3, 2015 from World Wide Web: http://www.rpdp.net/sciencetips_v2/P12C6.htm)

Transformers are static devices with high operating efficiency. The only component which reduced transformer efficiency is the total losses occurring on them. The losses are divided into two main subgroups. These are namely magnetic originated and electrical originated losses. Electrical originated losses are I^2R losses occurring on both primary and secondary windings. These are relatively straightforward losses to compute. The real challenge is to compute magnetic originated losses. For instance, eddy losses due to changing magnetic field generate circulating currents on both copper conductors and metallic parts. These losses are heavily dependent on conductor dimensions, temperature of conductor, the frequency and the thickness of the conductor. Another important loss occurs on magnetic path of the core. The core material shown in Figure 2, is grain oriented electrical steel, where the magnetic domains are subjected to sinusoidal magnetic flux. This will force magnetic domains to rotate. During this rotation, magnetic domains generate heat energy. Additionally, the changing magnetic field causes eddy currents in the core material according to Faraday's law. These two effects are called no-load losses and these losses occur only on magnetic path.

Figure 2. Transformer Core Steel.

The above mentioned no-load and load losses generate excessive heat on the transformer. The generated heat should be dissipated to the surrounding atmospheric medium in order to keep the hottest spot temperature below the allowed limit. This limit is dependent on the temperature class of the material used. In power transformers (Figure 3), natural cellulose based insulation materials are used due to their excellent electrical insulation properties. These insulation materials suffer from a process called

thermal aging. Thermal aging degrades the mechanical properties of the cellulose based insulation material and these materials become brittle over a certain temperature. Aging is basically an attack of OH components of transformer oil to cellulose fibers. Cellulose fibers become shorten as a result of this chemical process. This chemical process is function of temperature and for A Class insulation materials the temperature limit is 118˚C.

Transformers are cooled by using different cooling modes according to type and power of transformer. Transformer cooling systems have an important role in transformer life.

Figure 3. Power Transformer.

This study provides information and guidance to researchers who are interested in thermal and hydrodynamic analysis of transformers. The main aim of this study is to investigate of a transformer radiator with different transformer oil types to obtain the pressure difference with respect to velocity. Then, viscous resistance and inertial resistance coefficients can be obtained easily to study with porous medium approach. This study provides a detailed view and analysis about transformer radiators and the thermal behavior of different types of transformer oils.

General information about energy and transformer will be given in Chapter 1. Additionally, transformer losses and cooling modes were covered. Chapter 2 presents the studies on transformer life, reducing hot-spot temperature, further developments of new methods, comparison between CFD simulations and experiments, porous media approach in CFD simulations, complete and slice models, transformer winding and transformer cooling fluids. Overview of this study according to presented literature review was presented also in Chapter 2. Transformer oils and their properties were explained in Chapter 3. Then, numerical analysis that covers the methodology of this problem was discussed in Chapter 4. Problem statement, modelling, meshing, general settings, viscous model, material properties, boundary conditions and solution were considered in Chapter 4. Finally, Chapter 5 concludes this study by summarizing the results and discussion. Dimensionless numbers were calculated in Chapter 5. Also, correlation was developed between Reynolds number and Prandtl number to obtain Nusselt number. In conclusion, the aim of study was summarized. Additionally, further work developments were explained in conclusion chapter.

1.1. What is Transformer?

Transformers are electrical machines that transform alternating current energy from one voltage to another voltage without a change in frequency. The first developed transformer was designed in the early 1980s. The working principle of transformers depends on the Faraday's law of induction. Voltage is generated by moving the magnet near a wire according to Faraday's law. This voltage is called electromotive force (emf) and denoted ε. Electromotive force is directly proportional to the rate of change of magnetic flux.

Transformers can be grouped into two classes according to cooling method; oil-immersed transformers (Figure 4) and dry type transformers (Figure 5). In this study, heat transfer and fluid flow were investigated in a radiator of an oil-immersed transformer.

Figure 4. Oil-immersed Arc Furnace Transformer.

Air is used for transformer cooling in dry-type transformers. Air is directly forced into core and winding by using fans. This type of transformers have the power limits because their losses are higher. Air is used for cooling fluid to dissipate heat.

Figure 5. Dry-type Transformer.

The generated heat is dissipated through the cooling systems according to the transformer type. In oil-immersed transformers, excessive heat is dissipated through

transformer oil. The heat transfer from the conductors and the magnetic path is transmitted to the transformer oil by conduction and convection. The heat transfer by conduction is very small compared to convection heat transfer. The parameters that effects heat transfer are conductivity of the insulation materials, winding cooling duct dimensions, types of winding, disc width, spacer thickness, distance between discs, overall winding dimensions, thermal properties of transformer oil type and the velocity of transformer oil. The heat transmitted from windings to the transformer oil is circulated into transformer radiators. The heat transfer in the radiators is due to conduction, convection and radiation. Conduction heat transfer is extremely small compared to convection type heat transfer as shown in Figure 6. T_{oil} is the oil temperature that is circulating in radiator, T_{wall} is the temperature of radiator steel and T_{air} is the ambient temperature. On the other hand, radiation heat transfer is negligible in transformers according to literature.

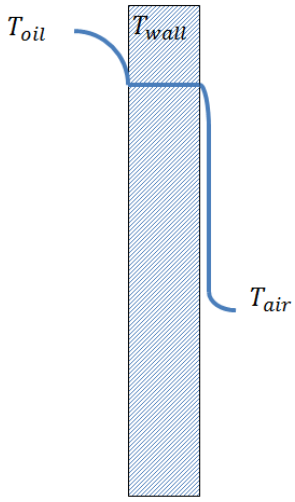

Figure 6. Heat Transfer at Radiator Section.

The aged insulation material becomes brittle and ruptures, if the generated heat is not dissipated to the surrounding medium. This exposes to conductor material to touch each other and two adjacent conductors short circuit. This generates excessive currents to flow between two conductors and the transformer explodes. This is a catastrophic failure accompanied with a fire.

Transformers consist of four main parts as core, winding, tank and accessories as shown in Figure 7.

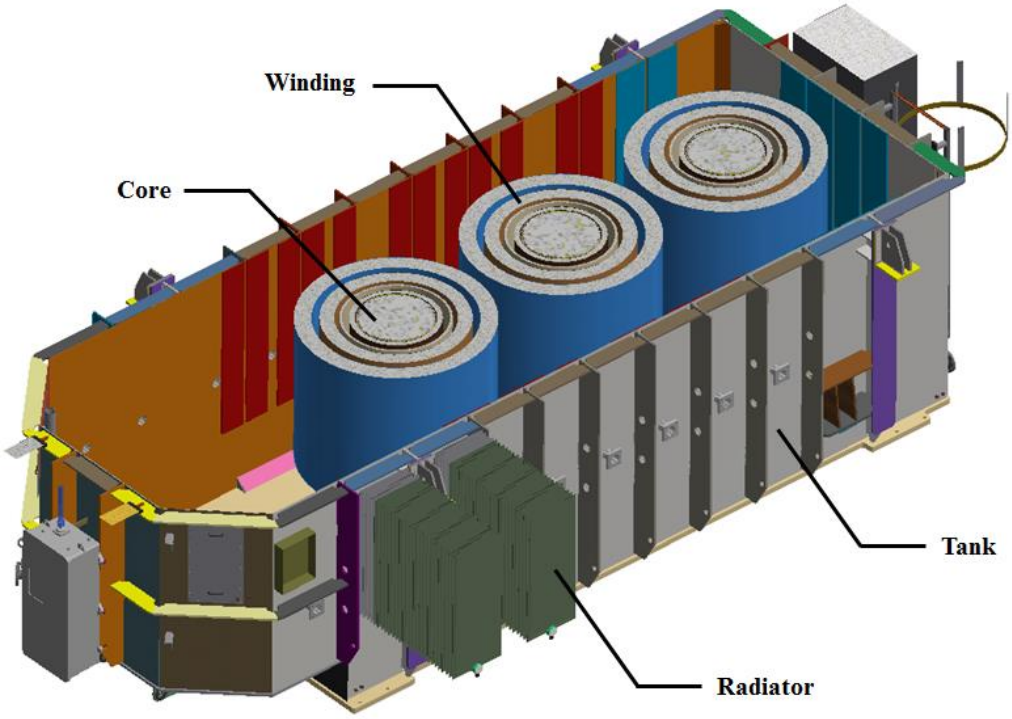

Figure 7. Transformer Main Parts.

1.1.1. Core

Magnetic flux is generated in winding by the current flowing through the windings. Transformer core is used to create a magnetic flux path (Figure 8). The core is laminated to reduce the eddy current losses in transformers (Figure 9).

Figure 8. Transformer Core.

Laminated silicon steel core is made up of insulated thin laminations. Silicon steel core provides low hysteresis loss and high permeability.

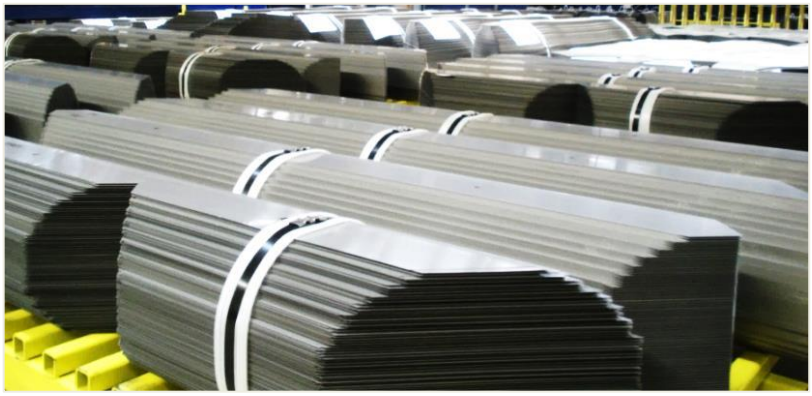

Figure 9. Laminated Coated Core.

Step-lap method is used to construct transformer core. Transformer core consists of steps and books as shown in Figure 10.

Figure 10. Step-lap and Books.

1.1.2. Winding

The winding is composed of the wire conductors as shown in Figure 11, which are wounded around the core, and these are covered with cellulose-based insulation material.

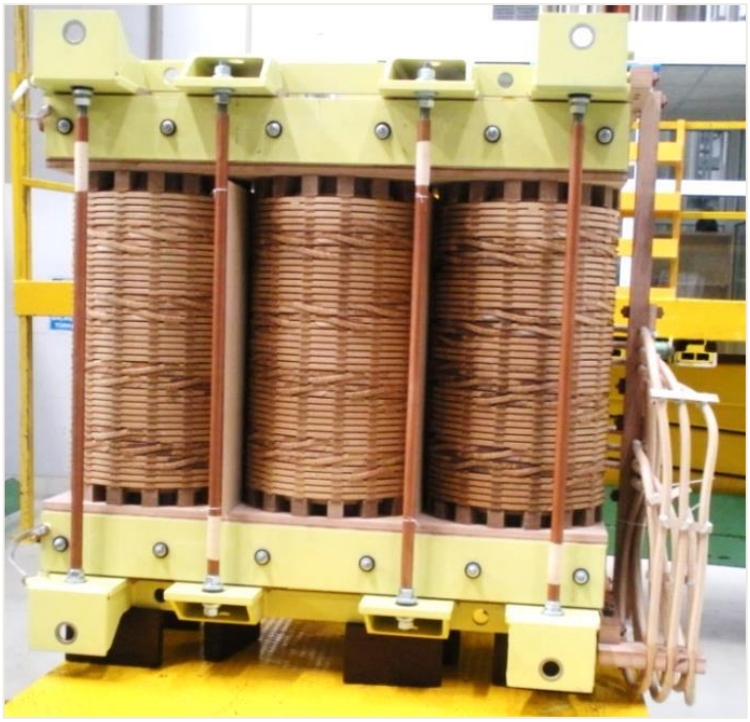

Figure 11. Transformer Winding.

Conductors are insulated to avoid electrical breakdown, creepage and partial discharge. Special paper is used for insulation of winding that is called insulation paper as seen Figure 12.

Figure 12. Winding Insulated Conductors.

The source of magnetic flux is primary winding. Magnetic flux tends to pass through the core that has high magnetic permeability. The relative permeability of transformer core material is nearly 20000 times higher than air. Thus, magnetic flux is induced to secondary winding. Windings and the core together forms the active part located in transformer tank. The main leakage field in transformers occurs between low voltage and high voltage windings. As a result, excessive eddy losses and eddy currents acts on these materials. In order to decrease the values of eddy currents, the transformer conductors are divided into many small pieces and each piece is isolated from neighbor conductors with special polymer based epoxies. This application helps reducing eddy current and loss values in windings. However, every divided conductor has to be transposed in order not to generate circulating currents due to resistive differences.

1.1.3. Tank

Transformer tank (Figure 13) is a mechanical element of transformer that provides a protection by surrounding transformer oil and active parts. Most of the transformer equipments are mounted on the transformer tank. Leakage magnetic fields generate circulating eddy currents on the tank wall. Therefore, appropriate magnetic shunts or magnetic screening has to be provided. Excessive heating will occur on the tank wall, if magnetic shunts or flux rejecters are not provided. The temperature due to these circulating currents can be as high as 300˚C locally. Therefore, conductors carrying high currents generates additional heat source in transformers.

Transformer tank is designed to withstand 2 bars of hydrostatic pressure. Considering a power transformer dimensions which can reach values as high as 12 meters special stiffeners has to be provided. Otherwise, large and permanent deflections occur on the transformer tank, which are not allowed according to IEC Standards.

Figure 13. Transformer Tank.

Corrugated tanks (Figure 14) are frequently used for distribution transformers as cooling fins. Transformer losses are dissipated through the corrugated walls. However, corrugated walls suffer from excessive internal pressure and limit the transformer sizes due to their low mechanical strength. On the other hand, due to their flexibility they can be work in a completely closed transformer design, namely hermetically sealed transformer. In this study, hermetically sealed transformer design was not focused on.

Figure 14. Corrugated Transfromer Tank.

1.1.4. Accessories

Tap changers, bushings, moisture holders, pressure safety valves, throttle valves, buchholz relay and thermometers are some of the transformer accessories as seen in Figure 15.

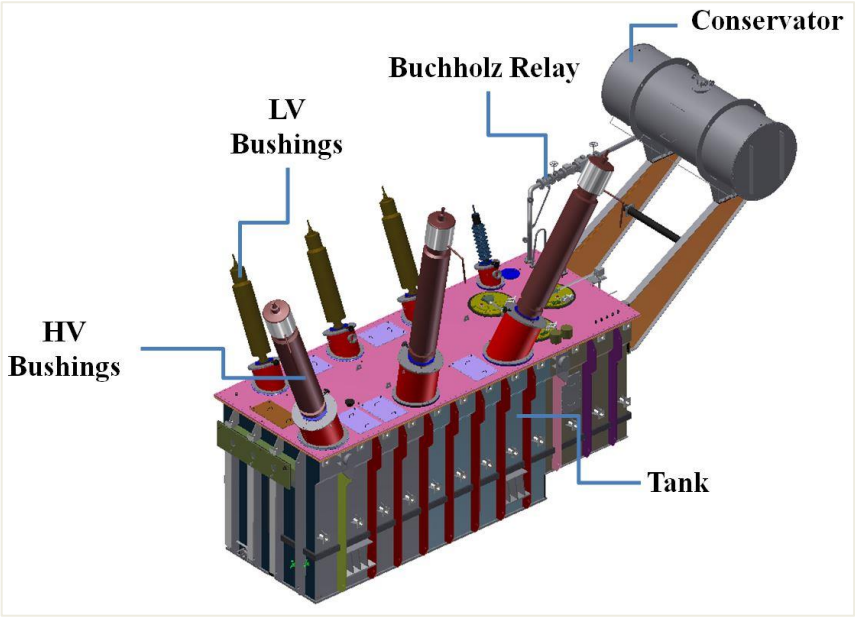

Figure 15. Transformer Parts.

1.2. Transformer Losses

Transformers are the kind of electrical machines that have energy losses as all electrical machines. Two main types of losses occur in transformers; copper losses and iron losses.

Copper losses are produced in transformer windings and defined with I^2R loss. Copper losses are the product of electrical currents in the conductors of the transformer windings. Hysteresis loss and eddy current loss are both iron losses that occur in core depending on ferromagnetic material properties. The magnetic flux passing through the core generates circulating eddy currents because of the Faraday's law of induction. This circulating current generate additional losses and heats up the core. As the cross-sectional area of core gets larger, the losses increase. In order to decrease of the amount of dissipated losses, the core builds up from very thin laminations. The surface of each lamination is coated. Thin and laminated iron sheets are used in transformer core to decrease the eddy currents.

1.3. Cooling Modes

Cooling modes in oil-immersed transformer will be explained in this part. Transformers work in specified temperature mentioned in loading guide for oil-immersed power transformers part (Part 7) of IEC 60076-7 International Standards (2005-12). All losses (iron losses and copper losses) are converted to heat energy in the transformer. Copper losses are the main source of the heat energy. The occurred heat energy increases the temperature of transformer. Transformer coolant is used to avoid overheating in transformer. Insulation paper is damaged by excess heat which is discarded by using transformer oil. Especially, radiators are used to increase the heat transfer surface area in power transformers. Fans and pumps are also used in power transformers as shown in Figure 16 that cannot be cooled using only radiators. Fans are used to drive the air on the radiator outside surfaces and pumps are used to circulate the oil into transformer tank or radiators.

Figure 16. Transformer with Radiators and Fans.

The generated heat in the core and winding is transferred to the oil inside the transformer. Transformer cooling systems are classified with four letter designation. The first letter indicates the type of cooler. Second letter is to show whether the cooler circulates natural or forced. Third letter designates the type of cooler that moving on the outer cooling surfaces. The fourth letter shows the circulation type for the cooler moving on the outer surfaces. The main types of cooling modes for oil-immersed transformers can be listed as below in Table 1 and Table 2.

Table 1. Transformer Coolant Types.

Cooling Type	Symbol
Oil	O
Gas	G
Water	W
Air	A
Solid	S

Table 2. Circulation Types.

Circulation Type	Symbol
Natural	N
Forced	F
Directed	D

1.3.1. ONAN (Oil Natural - Air Natural)

ONAN cooling mode is the basic cooling system in oil-immersed transformers. The heated fluid flows upward and flows into the radiator from the inlet as shown in Figure 17.

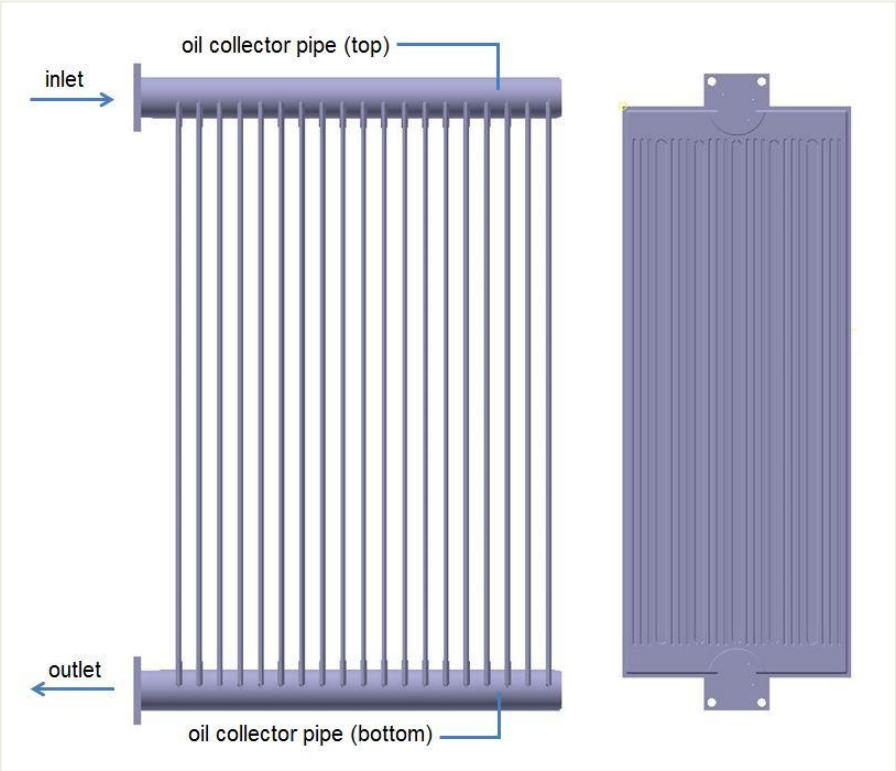

Figure 17. Radiator.

Oil flows through the radiator ducts and cooled oil is entered into the tank (Figure 17). Oil is circulated in the space of winding and core. Air flows through the outside surfaces of the radiators by natural convection. Also, oil collector pipes are shown in Figure 18. Oil is collected from the upper oil collector pipe into radiator. Then, cooled oil is transmitted into tank from the bottom oil collector pipe. Circulating

oil in transformer and radiator is very slow in ONAN mode. Basically, the principle of thermosiphon effect provides the circulation of transformer oil in transformer and radiator. Temperature difference between the transformer oil in tank and transformer oil in radiator causes pressure difference, then this pressure difference circulates the transformer oil.

Figure 18. Transformer Radiators.

1.3.2. ONAF (Oil Natural - Air Forced)

In ONAF mode, fans are blown to the cooling surfaces whereas the oil circulates naturally inside the radiators. Fans are generally mounted below of the radiators. The air flow rate is higher than air natural mode. ONAF mode is mostly used in power transformer. ONAN/ONAF cooling modes combination can be also used in transformers. In this type of cooling mode, natural cooling is used up to certain load. Fans are worked automatically when the load exceeds the certain loads. Heat dissipation rate in ONAF mode is higher than ONAN mode.

1.3.3. OFAF (Oil Forced - Air Forced)

Pumps and fans are used to move coolant in OFAF mode. Oil is forced to circulate in the transformer. Air is forced by using fans for cooling purposes of the circulated oil.

1.3.4. ODAF (Oil Directed Air Forced)

Oil is directed into the winding and air blowing is obtained by using fans in ODAF mode. Directed oil flows in oil ducts of winding. ODAF mode is generally used in high rate power transformers.

Figure 19. Transformer and Radiators.

Kulkarni and Khaparde (2005) remark the static electrification in large power transformers. Higher the pump capacity the higher the heat transfer rate trend was used until the some power transformers failed by static electrification phenomenon. Static electrification phenomenon depends on moisture content of transformer oil, temperature, flow rate, turbulence, surface conditions, pumps, orifices and AC/DC fields. Therefore, pump selection in OFAF and ODAF cooling modes has an important role in power transformer design. Consequently, higher the pump capacity does not mean the higher heat transfer rate.

Additionally, OFAF and ODAF cooling modes are explained by Kulkarni and Khaparde (2005). Transformer oil is forced into transformer tank in OFAF cooling mode, while it is directed into the winding in ODAF cooling mode as seen in Figure 20.

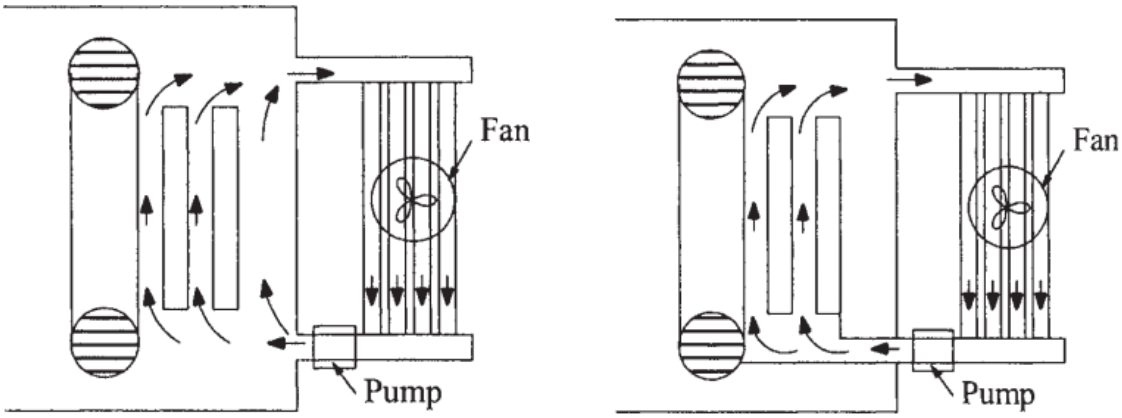

Figure 20. OFAF (left) and ODAF (right) Cooling Modes.
(Source: Kulkarni and Khaparde, 2005)

CHAPTER 2

LITERATURE REVIEW

This chapter will explore the literature that is relevant to understanding the importance of thermal and hydrodynamic studies on the transformers. Each section will summarize the main point of studies respectively. Transformer life, reducing the hot-spot temperature, further developments of new methods, comparison between CFD simulations and experiments, porous media approach in CFD simulations will be covered. Furthermore, a study with complete and slice models is reviewed in this chapter. Then, some of the studies on transformer winding hot spot temperature were presented. Many studies have been performed regarding the thermal behavior of transformer winding that has been presented in this chapter. On the other hand, not many researches have been found in the literature on the thermal and hydrodynamics behavior of transformer cooling systems. Thermal and hydrodynamic studies in transformer winding will be investigated in the light of this study in the near future. In this respect, this study plays an important role in characterization of thermal and hydrodynamic properties of transformer cooling systems.

Oil-immersed transformers are preferred that have dielectric oil for cooling and insulating as noted by Fernández et al. (2012). Mineral oil that has been widely used in the power transformers, although is not biodegradable. Studies about transformer oils and alternative cooling fluids are presented in this chapter.

2.1. Transformer Life

Winding temperature must be kept below a certain temperature limit, because the excess heat in the windings directly accelerates the aging of insulation material. Transformer life depends considerably on the aging of this cellulose-based insulation material in winding.

Wittmaack (2014) was stated that chemical degradation in the electrical insulation affects transformer life. Load losses were calculated by using Maxwell electromagnetic field simulation software. The study aims at predicting the temperature

distribution on cellulose based and nomex insulating materials with CFD. The steady-state CFD model used in the analysis contains curvilinear, non-orthogonal block structured mesh elements. Temperature dependent material properties have been utilized. Continuity, momentum and energy equations were solved by SIMPLE, SIMPLEC or PISO algorithms. The study did not give any solid conclusions occurring on insulation materials but mentions that pressure drop and temperature distribution can be obtained. Figure 21 shows the temperature distribution on radial spacers.

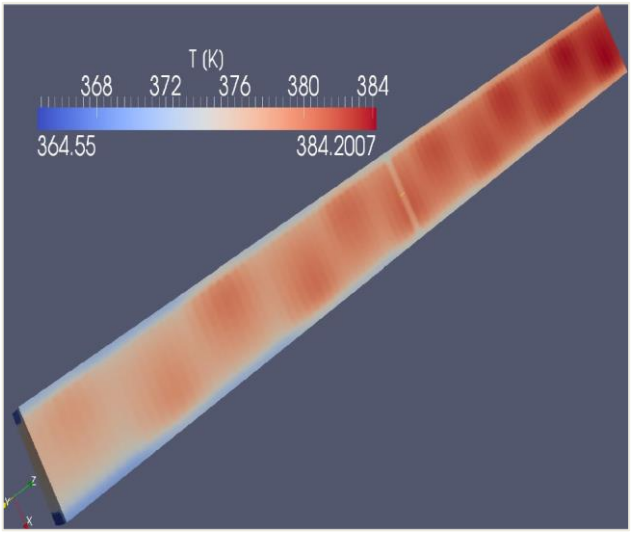

Figure 21. Temperature Distribution on Radial Spacers.
(Source: Wittmaack, 2014)

2.2. Reducing the Hot-spot Temperature

CFD simulations have an important role in power transformer design, because of the limitations of experimental measurements. Normal life expectancy of a power transformer is about 20 years. Fonte et al. (2011) stated that the hot-spot temperature can be reduced by as much 10˚C which has a strong direct impact on the power transformer's lifetime. 2D axis-symmetric CFD models were simplified. Flow and heat transfer equations were solved by using Fluent 6.3 from ANSYS Inc. Power transformers working with ODAF and ONAF cooling systems were simulated in this study. Both 2D and 3D models were generated for ODAF cooled transformer model. Hydrodynamic and thermal effects of radial spacers were not taken into account. 800000 elements were used with mesh refinement to construct grids in 2D CFD model. On the other hand, 3D model was simulated with using 2450000 tetrahedral/hexahedral

elements. Only the 2D computational grid was created for ONAF cooled transformer. Naphthenic oil was used as coolant in this power transformer and small temperature difference within the oil was investigated. Boussinesq model was used to specify density for the natural convection flow. Then, the calculated equation of temperature based density is seen as below.

$$\rho = 868[1 - 6.40 \times 10^{-4}(T - 293)] \quad (2.1)$$

where ρ is used to indicate density of naphthenic transformer oil in kg/m^3 and T is the temperature in K.

Measurements of viscosity were performed by using cone/plate rheometer in the temperature range 20˚C to 80˚C. Then, temperature based viscosity equation was obtained as shown below.

$$\mu = 1.43 \times 10^{-7} \exp\left(\frac{3480}{T}\right) \quad (2.2)$$

where μ is the viscosity of the naphthenic transformer oil in Pa·s and T is the temperature in K. Moreover, specific heat capacity and thermal conductivity were assumed constant as $c_p = 2016\ J\ kg^{-1}K^{-1}$, and $k_{oil} = 0.126\ W\ m^{-1}\ K^{-1}$, respectively.

Disc model was simplified using calculated equivalent thermal resistance. Simulations were studied with using two types of conductors to validate simplified conduction model. Rectangular bar was used in Type 1 and copper transposed cable was used in Type 2 as shown in Figure 22. The difference between detailed and simplified disc model in both types was obtained as around 10% as seen in Figure 22.

Different boundary conditions were identified for both ODAF and ONAF cooling systems. Boundary conditions were used equal for ODAF cooled transformer at the inlet and outlet in 2D model simulations and the flow rate was obtained by describing the pressure difference. On the other hand, flow rate was increased by the pressure drop along the spacers in 3D disc model.

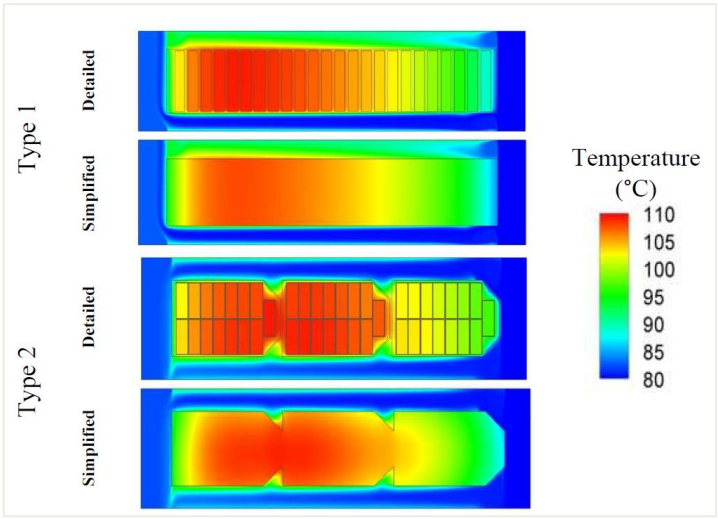

Figure 22. Temperature Distribution of Detailed and Simplified Disc Model for Two Types.

(Source: Fonte et al., 2011)

For ONAF cooling systems, where the oil flows by natural convection, pressure is corrected at boundary conditions with calculating height-dependent density value.

$$\rho = \rho_0[1 - \beta(T_{inlet} + \alpha h - T_0)] \tag{2.3}$$

where ρ is the density, ρ_0 is the density of oil at the reference temperature, T_0 is the reference temperature, h is the height, α is the slope of temperature rise, T_{inlet} is the inlet temperature of the winding and β is the oil thermal expansion coefficient. Pressure drop between the inlet and outlet was calculated as shown below.

$$\Delta P_{relative} = \int_{h_{inlet}}^{h_{outlet}} \rho g dh - \rho_{op} g(h_{outlet} - h_{inlet}) \tag{2.4}$$

According to the obtained results, 3D model was gave the best estimate for the experimental temperatures. As a result of this study, the position and magnitude of the hot-spot were determined on the third disc from the top as shown in Figure 23. As seen in this study, CFD simulations of transformers provide many advantages.

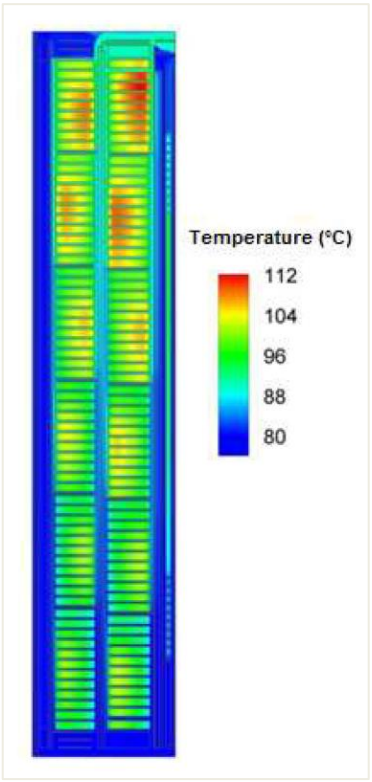

Figure 23. Temperature Distribution of Disc for the 2D Model.

(Source: Fonte et al., 2011)

Deviations were observed in both ODAF and ONAF cooling system because of the using of a simplified heat conduction model.

2.3. Further Developments of New Methods

Simplified network approach is used for thermal design in literature. Joshi and Deshmukh (2004) claimed that a new method used in developed new software is more accurate than conventional method to define oil rise and winding rise. Temperature based oil properties were defined at each node in network. Transformer winding was modelled as disc and crossover winding. Oil guiding washers (OGW) are used to direct oil flow in winding. Oil and air are circulated naturally in ONAN cooling system whereas air is forced with fans in ONAF. In addition, oil is forced with using pump in OFAF. The effects of fans and pumps were investigated. Radiators were modelled as flat plated to simplify calculations in this study. Therefore, flow of oil in radiators cannot be examined. Tank walls were also modelled as flat plates. Indeed, this study was focused on the oil flow in winding. The methodology of thermal predictions of the

complete transformer model is discussed in this study. Average winding rise, top oil rise and hot spots were predicted with different cooling systems for instance, ONAN, ONAF and OFAF. Heat is transferred to air by both convection and radiation. Total heat transfer is found by summing convection heat transfer and radiation heat transfer.

$$Q_{total} = Q_{convection} + Q_{radiation} \quad (2.5)$$

The external air flow was determined as laminar in the initial part of fin surfaces according to calculated Reynolds number and the flow was followed by turbulent flow.

Heat is transferred from the tank and fins surfaces slowly, for this reason they were assumed as isothermal surfaces. Pressure drop of oil moving toward the bottom collector pipe increases inside the oil ducts of fins. Unlike the radiator cooling system, oil pressure decreases with moving upwards in tank.

Moreover, buoyancy and pump create flow inside the windings. Network model was used to calculate pressure drop and oil temperatures in winding. Pressure decreases along the winding ducts by the effects of gravity, friction and bends. Local heat transfer coefficient was calculated with using average temperatures and velocities around disc. In some ducts, reversed oil flow was observed, then it was verified with using ANSYS CFD simulation software. Calculated disc temperatures were used to determine the average winding temperature in this study by using an iterative method. According to this study, this new method is more confident than conventional method. At this point, it is obviously clear that transformer cooling calculations should be improved with new methods.

2.4. Comparison Between CFD Simulations and Experiments

Verification and validation are the most important processes to increase confidence in CFD simulation. There is an example study from literature examined that ONAN and ONAF cooling system with experiments. Cooling performance of radiators used in oil-filled power transformers was studied with using two kinds of cooling system by Kim et al. (2012). ONAN and ODAF cooling systems were used to investigate the effects of non-direct and direct-forced oil flow. This study consists of

detailed calculations, CFD simulations and experimental results. Simulation was modelled with 4 radiators that each has 40 fins as shown in Figure 24.

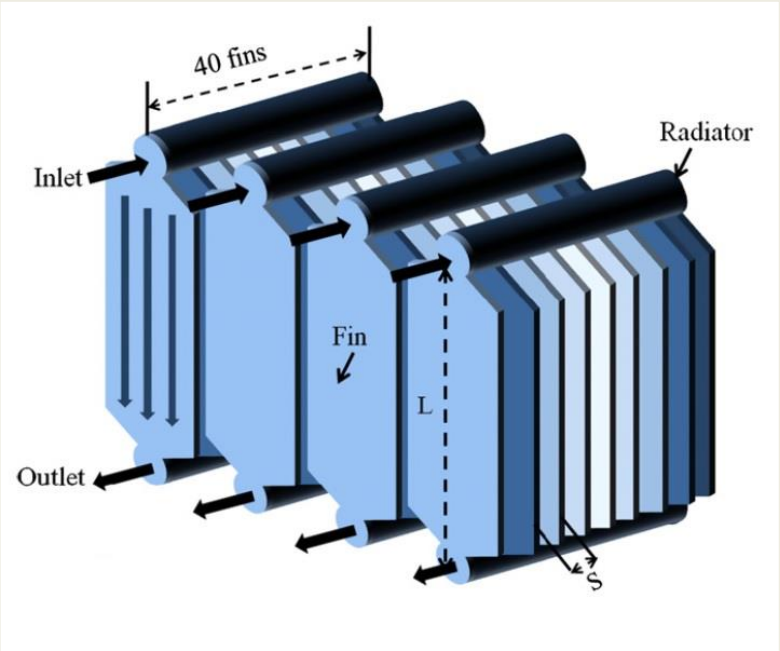

Figure 24. Radiator Model.
(Source: Kim et al., 2012)

Center to center length of each fin is indicated by L, which is equal to 3300 mm and gap between fins are indicated by S, which is equal to 45 mm. The oil volume flow rate was varied in the range from 1.0×10^{-3} m^3/s to 2.0×10^{-3} m^3/s.

Inlet temperature of radiator was assumed to be equal to the hot-spot temperature. Calculations of the temperature distribution and cooling capacity were verified with CFD simulations. Flow rate, inlet temperature and outlet temperature were measured, then compared with calculations and the CFD simulation results for both cooling methods.

Kim et al. stated that, temperature difference between inlet and outlet decreases as an increasing in flow rate. Thus, this work is obviously showed that the cooling capacity increases at high flow rate as shown in Figure 25.

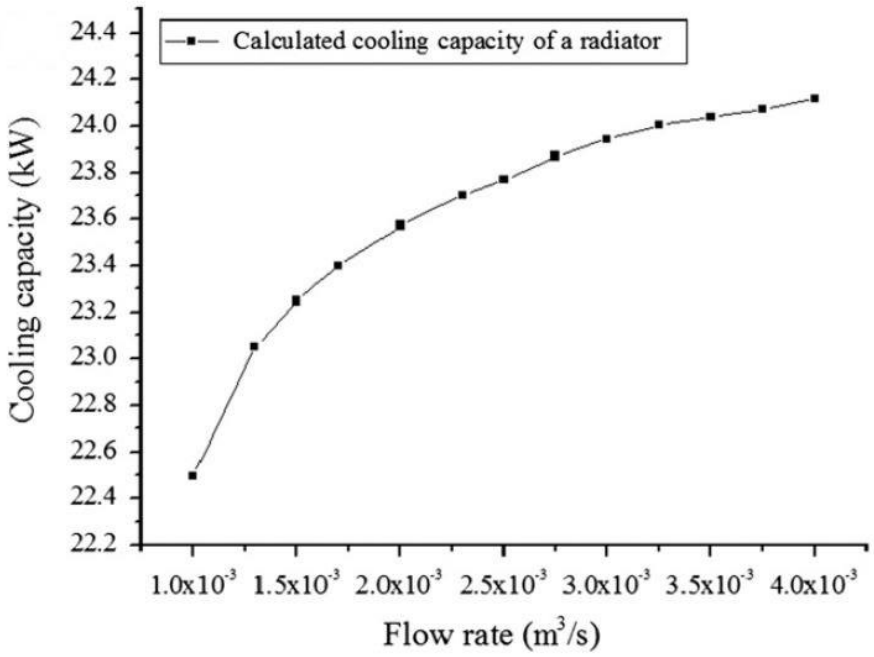

Figure 25. Cooling Capacity versus Flow Rate.

(Source: Kim et al., 2012)

Oil temperature increases at the distance from radiator top to bottom by increasing in oil flow rate. Temperature versus distance graph with different flow rates is shown below. As shown in Figure 26, it is seen that the oil temperature is higher for $4.0 \times 10^{-3} \mathrm{m}^3/\mathrm{s}$ flow rate at the same distance. Although the flow rate was defined up to $2.0 \times 10^{-3} \mathrm{m}^3/\mathrm{s}$, higher flow rate $4.0 \times 10^{-3} \mathrm{m}^3/\mathrm{s}$ was obtained by using a pump.

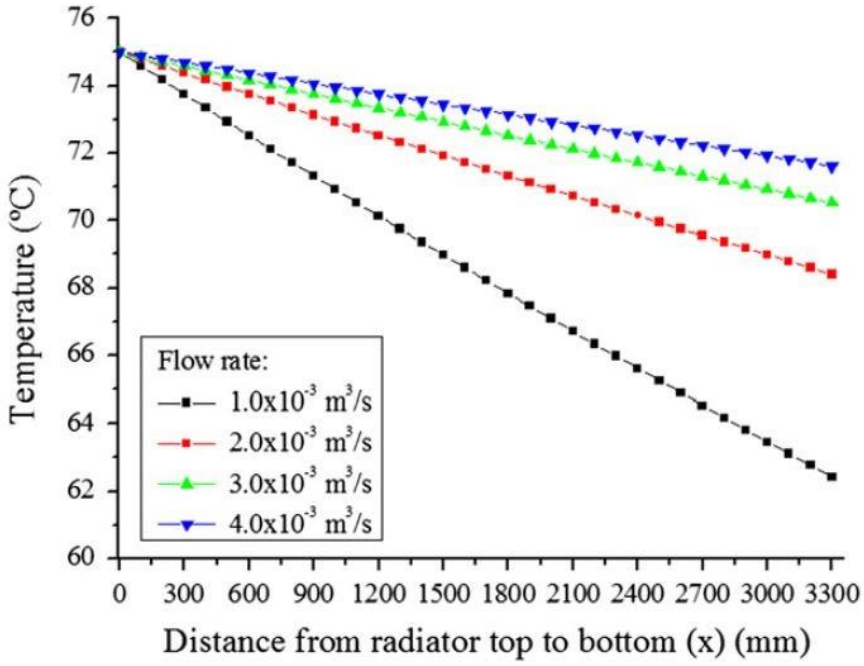

Figure 26. Temperature versus Distance From Radiator Top to Bottom.

(Source: Kim et al., 2012)

The total heat transfer coefficient was calculated using equation as shown below in Equation (2.6).

$$P_{total} = \sum_{N=1}^{40} P_{fin}(N) = \rho c_p Q_{oil}(T_{top} - T_{air})\left(1 - e^{-(h_p)}\right) \qquad (2.6)$$

where P_{fin} is the cooling capacity of a fin, P_{total} is the cooling capacity of the total cooling capacity of a radiator, which have 40 fins. ρ and c_p are the material properties of oil, which are dependent on temperature. Q_{oil} is indicated the oil volume flow rate.

Grid independent study is important for CFD simulations. Grid independency was studied by using same boundary conditions to verify the accuracy of the results. Over 7.3 million elements were used, then 8 million was chosen according to the result of the grid independency study.

Flow was defined as steady state and incompressible. Viscous model was constructed with using standard k-ε model. Boundary conditions were specified as mass flow rate at the inlet and out flow at the outlet. Inlet temperature was set up 75˚C. The convergence criteria were defined as under 1.0×10^{-6}. Outlet temperature was gained at 60.39˚C with $1.0 \times 10^{-3} m^3/s$ volume flow rate and 69.67˚C with $4.0 \times 10^{-3} m^3/s$

volume flow rate as shown in Figure 27 and Figure 28. Also, temperature distributions at the given volume flow rates are seen in Figure 27 and Figure 28.

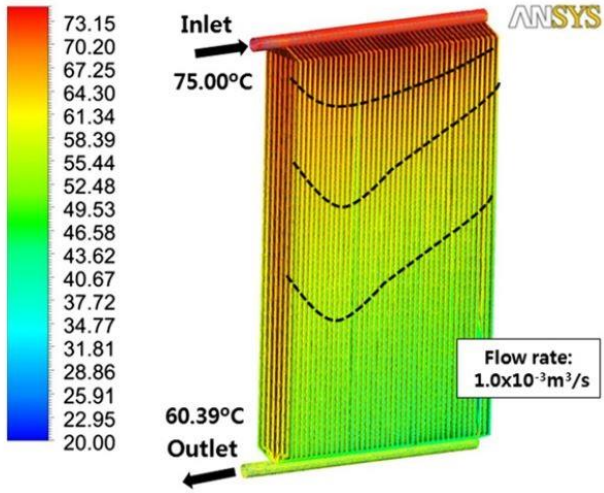

Figure 27. Temperature Distribution at the Flow Rate of 0.001 m^3/s.
(Source: Kim et al., 2012)

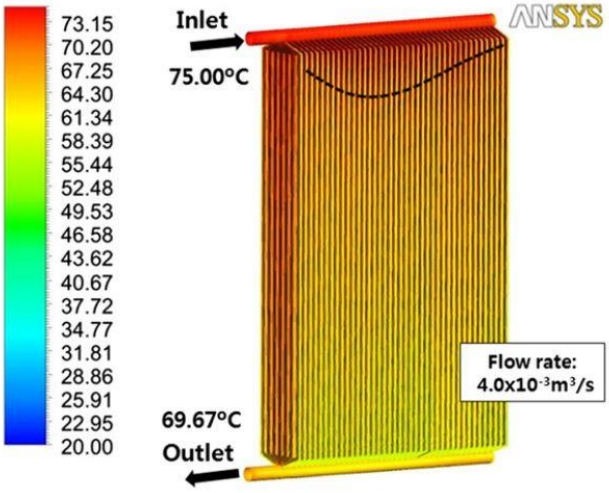

Figure 28. Temperature Distribution at the Flow Rate of 0.004 m^3/s.
(Source: Kim et al., 2012)

In experimental studies, T-type temperature sensors and ultrasound wave based flow sensors were used to measure inlet temperature (T_{inlet}), outlet temperature (T_{outlet}) and oil volume flow rate (Q_{inlet}).

There seems to be a general agreement between the analytical results and the experimental results, and as a result, theoretical calculations are verified with experimental studies.

2.5. Porous Media Approach in CFD Simulations

CFD model of power transformer requires a large number of mesh cells. Power transformer is modelled with using porous medium approach to decrease solution time, which is proportional to the number of mesh. Fdhila et al. (2011) focused on oil and air flows and the heat transfer in fan-cooled transformer radiators with using ANSYS Fluent 12.0 CFD simulation software. Symmetry boundary condition was used to model of the radiator groups. Fans were modelled as a volume in this study. The effect of fan position, fan size and oil flow rate were examined. The fan diameter varied between 0.8 m and 1.5 m. CFD model was simulated with using two, three and four fans. Temperature distribution in the radiators with three fans is shown in Figure 29 below. Air relative temperature distribution is showed at the left side and oil relative temperature distribution is showed at the right side in the radiators.

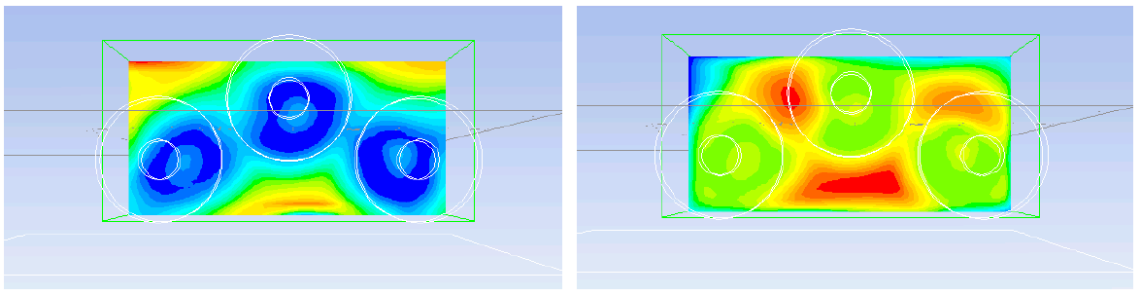

Figure 29. Temperature Distribution in the Radiators.
(Source: Fdhila et al., 2011)

Four different configurations were studied to determine the temperature differences between the inlet and the outlet of the radiators as shown in Figure 30. The effects of the fan size and the locations on the temperature difference were also analyzed. As a consequence, this research suggested that the porous medium approach provided decrease in solution time.

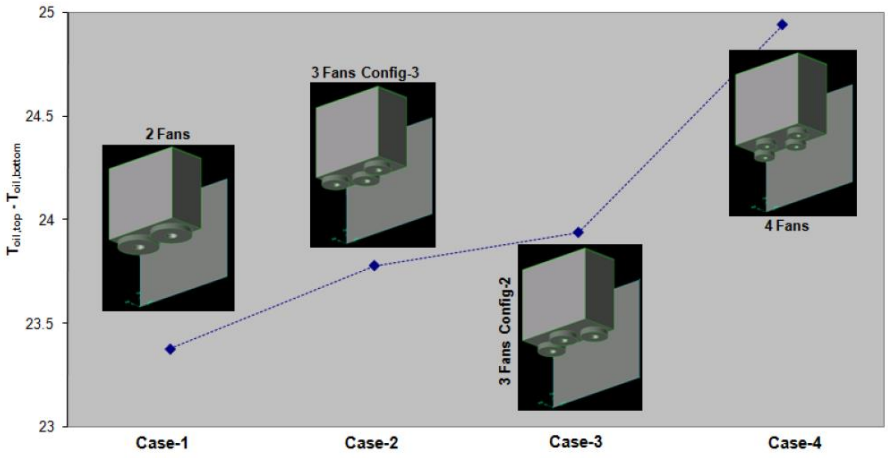

Figure 30. Temperature Difference (T_(oil,top) – T_(oil,bottom)) for Different Fan Configurations.

(Source: Fdhila et al., 2011)

2.6. Complete and Slice Models

Gastelurrutia et al. (2009) studied on distribution transformers with corrugated walls cooling ONAN (Oil Natural – Air Natural). Fluent V.6.3 software was used implementing the CFD codes. Three geometries for ONAN cooling system of distribution transformers were presented. First model (Trans-01) was handled 630 kVA. Second model (Trans-02) was smaller than first model and the corrugated wall was consisted more external fins. On the other hand, third model (Trans-03) was bigger and had more and longer fins. Low voltage and high voltage coils and channels were modelled with complete and slice models. Different flow domains and porous zone were used as shown in Figure 31.

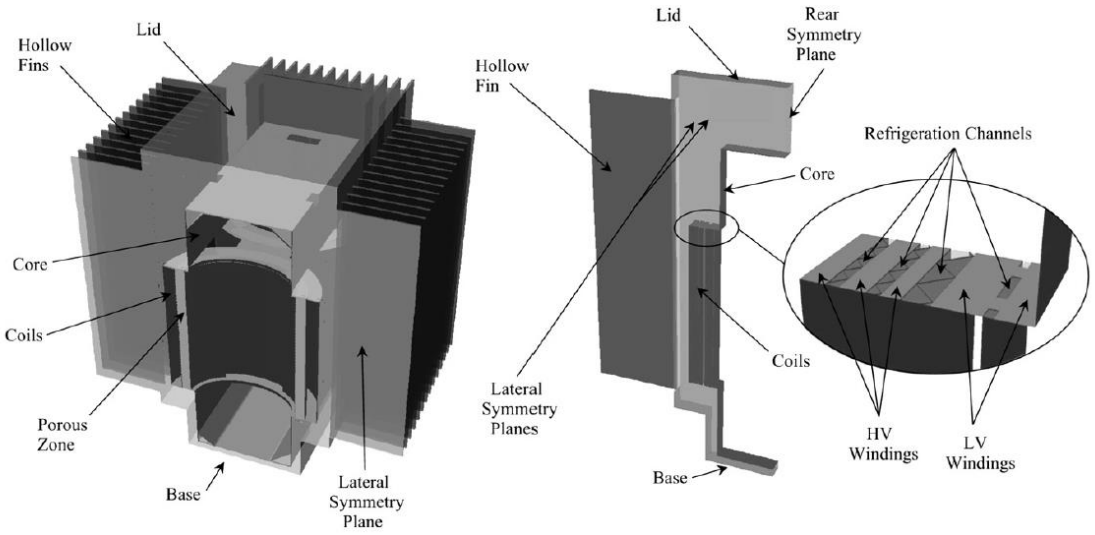

Figure 31. Developed Flow Domains for Second Transformer with Complete (left) and Slice Model (right).

(Source: Gastelurrutia et al., 2009)

Temperature was measured for each model with different power losses as shown in Table 3. The hottest surface was measured on the upper internal part of the fins (T9) in Figure 32. On the other hand, the coldest point was measured at the base of the transformer (T7) in Figure 32. In addition, temperature differences were evaluated according to the experimental measurements. Temperature difference in the vertical direction on the fins was calculated 14 K, and 2.5 K in the horizontal direction.

Table 3. Experimental Temperature Measurements.

	Transf-01			*Transf-02*	*Transf-03*
	$P_{N,1}$ [a]	$^3/_4$ $P_{N,1}$	$^1/_2$ $P_{N,1}$	$P_{N,2}$ [b]	$P_{N,3}$ [c]
$T_{ambient}$ (°C)	24.8	24.2	22.9	22.0	14.6
$\Delta T_{fin\ outlet}$ (°C)	22.3	17.0	12.4	–	–
ΔT_{oil} (°C)	51.4	41.8	31.5	46.6	56.2
ΔT_1 (°C)	46.8	38.3	29.4	46.1	53.6
ΔT_9 (°C)	49.5	40.5	30.5	46.9	54.5
ΔT_{10} (°C)	47.1	38.6	28.9	44.5	49.5
ΔT_{11} (°C)	44.8	36.4	26.9	43.1	44.8
ΔT_{12} (°C)	44.4	36	26.7	42	43.9
ΔT_{13} (°C)	35.8	28.6	20.3	31.7	34.9
ΔT_{14} (°C)	34.2	27.2	19.6	30.7	32.6
ΔT_7 (°C)	13.2	11.2	8.4	17.7	18.4

[a] $P_{N,1}$ means nominal power losses under normal operating conditions for *Transf-01*.
[b] $P_{N,2}$ means nominal power losses under normal operating conditions for *Transf-02*.
[c] $P_{N,3}$ means nominal power losses under normal operating conditions for *Transf-03*.

(Source: Gastelurrutia et al., 2009)

K-type thermocouples were used to measure the temperatures located on the external surface of the transformer as seen in Figure 32. Also complete and slice models are seen below. Radiation was neglected while the measuring temperatures.

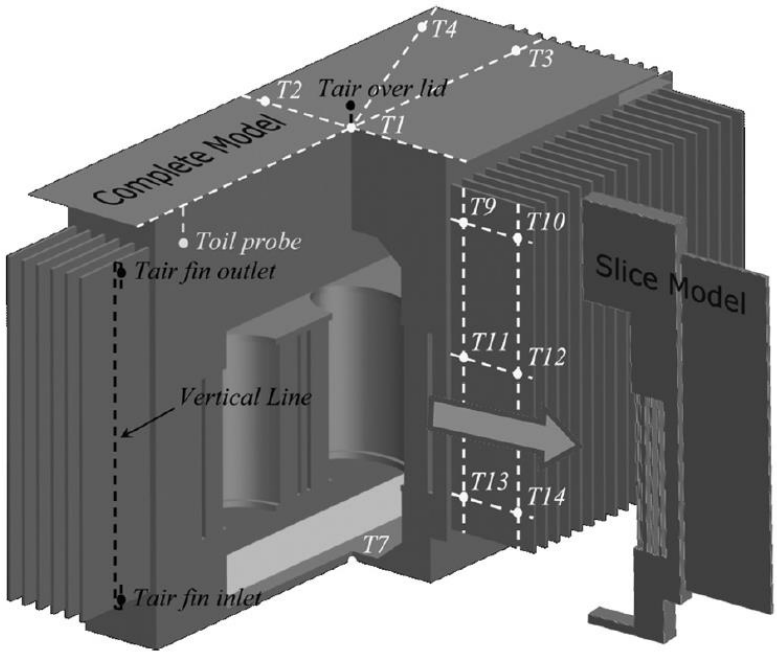

Figure 32. Position of the Thermocouples During the Experimental Tests and Geometry of the Complete and Slice Model.
(Source: Gastelurrutia et al., 2009)

Temperature differences between the complete and slice models for two different transformers (Transf-01 and Transf-02) were presented by Gastelurrutia et al. as shown in Table 4. Temperature difference between lid (T1) and the central fin (T11 and T12) was calculated as 1-2˚C. Also, 15-20˚C temperature difference was observed at the base of the transformer (T7).

Table 4. Comparison Between Complete and Slice Models.

	Transf-01 ($P_{N,1}$)			Transf-02 ($P_{N,2}$)		
	Complete	Slice	Dif.	Complete	Slice	Dif.
$T_{ambient}$ (°C)	25	–	25	–		
ΔT_{oil} (°C)	64.6	66.0	−1.4	51.2	52.6	−1.4
ΔT_1 (°C)	60.0	61.2	−1.2	46.8	49.0	−2.2
ΔT_9 (°C)	62.6	63.7	−1.1	49.5	50.9	−1.5
ΔT_{10} (°C)	62.3	63.2	−0.9	48.8	50.3	−1.6
ΔT_{11} (°C)	61.2	62.1	−0.9	47.5	48.6	−1.1
ΔT_{12} (°C)	61.2	62.1	−0.9	47.4	48.8	−1.3
ΔT_{13} (°C)	59.1	58.7	+0.4	44.6	43.0	1.6
ΔT_{14} (°C)	59.0	58.6	+0.4	44.4	42.8	1.6
ΔT_7 (°C)	49.8	28.5	+21.3	35.6	17.4	+18.3

(Source: Gastelurrutia et al., 2009)

The model of hollow fins was divided into 3 zones for each transformer model as shown in Figure 33 below. Uniform temperature distribution was obtained at the first zone, while temperature distribution was increasing in the second zone linearly. Then, the sharp temperature drop was shown at the bottom part of the fins.

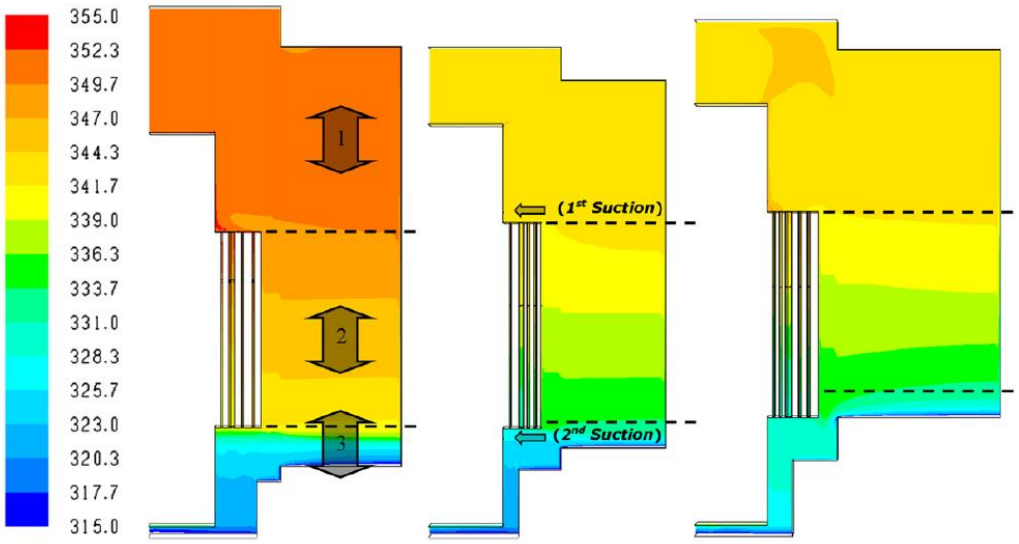

Figure 33. Oil Temperature Distribution in a Vertical Mid-plane of the Fins in Kelvin: Transf-01 (left), Transf-02 (middle), Transf-03 (right).

(Source: Gastelurrutia et al., 2009)

Gastelurrutia et al. evaluated the influence of turbulence modelling. Furthermore, grid independence was verified and the external thermal boundary conditions were carried out. It was observed that the heat transfer coefficient varied in the vertical direction.

2.7. Transformer Winding

In many research, thermal and hydrodynamic performance was studied in transformer winding by researchers. The most important parameter is the hot spot temperature in transformer design. Hot spot is the highest temperature occurred in the winding and the primary reason for ageing of insulation materials. Ageing is a direct function of temperature that occurs on transformers and IEC Standards defines the aging rate of a transformer as a function of temperature. Winding is the heat source of the transformer and that heat is dissipated by cooling equipments.

Radakovic and Sorgic (2010) were studied on the basics of detailed thermal-hydraulic model for thermal design of oil power transformers. They were presented the method for the calculation of temperatures inside the oil immersed power transformers, based on detailed thermal-hydraulic model for natural, forced and directed oil flow. Calculation safety factors can be reduced by accurate calculations. Therefore, cost of production can be also reduced.

Skillen et al. (2011) were dealt with transformer losses and cooling modes for the low-voltage winding geometry which has been considered. Also, the effect of inlet mass flow rate on the solution has been investigated. It was found that the significant local hot-spots were predicted via the use of CFD tools.

El-Wakil et al. (2006) performed a simulation of a step-down transformer including core and windings by using Fluent Software. PISO (the pressure-implicit with splitting of operators) method was used to solve equations. The inlet oil temperature of winding was 338 K. They were focused on the cooling optimization of the power transformer. Different geometries were simulated with six different flow rates of the cooling oil at the entrance of winding as shown in Figure 34.

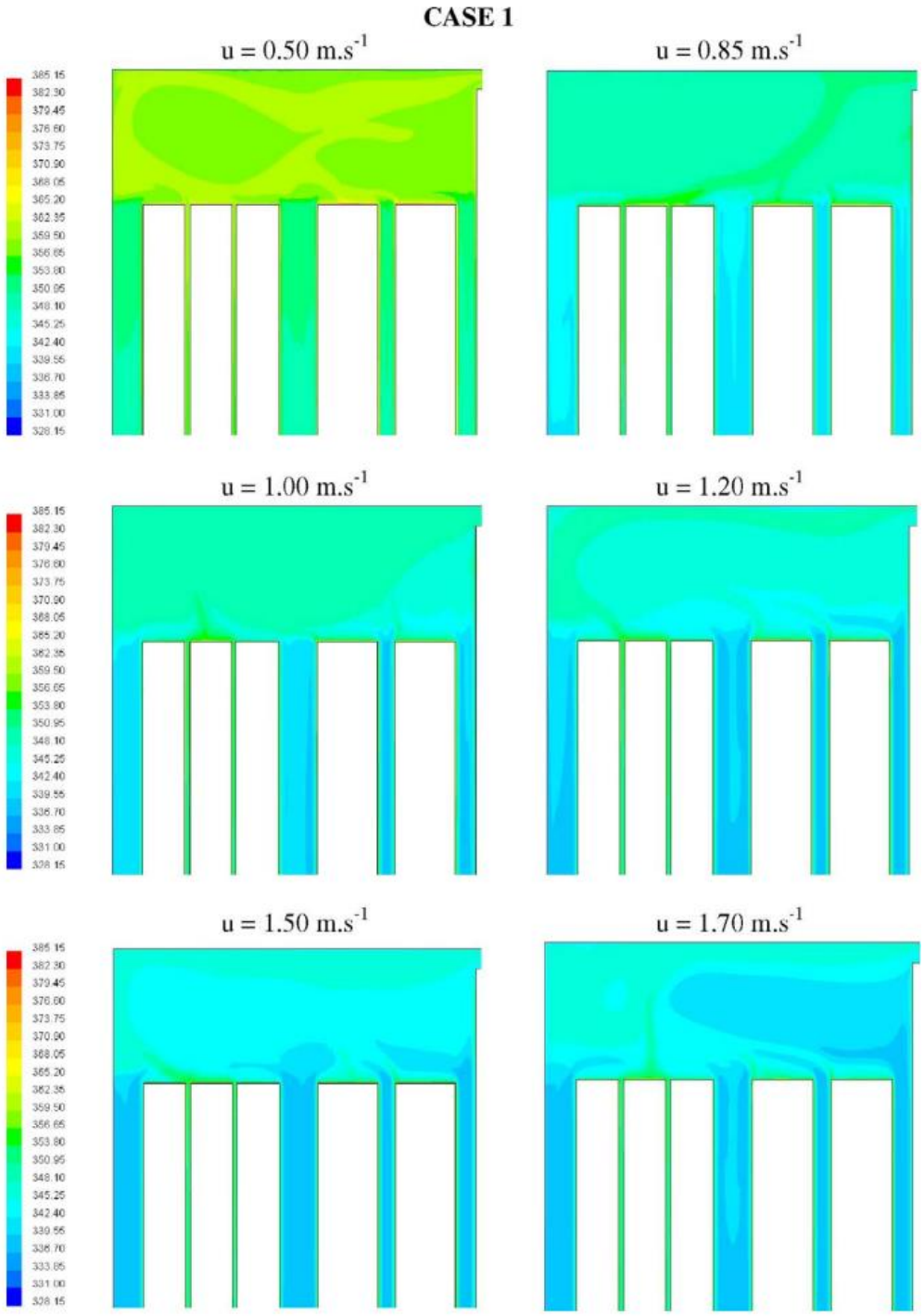

Figure 34. The Isotherms at the Top of Transformer for Different Inlet Velocities. (Source: El Wakil et al., 2006)

Heat transfer and fluid flow inside the winding oil cooling channels were studied by using numerical method with six different cases. Finally, Case 1 was obtained as the best geometry configuration, which has no insulations.

2.8. Transformer Cooling Fluids

Transformer oil is used for the purpose of cooling and insulating medium in oil-immersed transformers. Generally, three types of transformer oil are used; mineral oil, ester oil and silicone based oil.

Concern about contaminating effects of transformer oil on the environment is increasing day by day. In this respects, researchers are focused on the alternative fluid that will replace mineral oil in recent years. Fernández et al. (2012) compared main properties of alternative fluids for power transformers. Mineral oils are widely used in oil-immersed transformers although they are not environmentally friendly and they contain high risk of fire. They classified the insulating fluids into four group; mineral oils, high molecular weight hydrocarbons (HMWH), silicones and ester-based fluids. In addition, miscibility of alternative fluids were presented as shown in Figure 35 below.

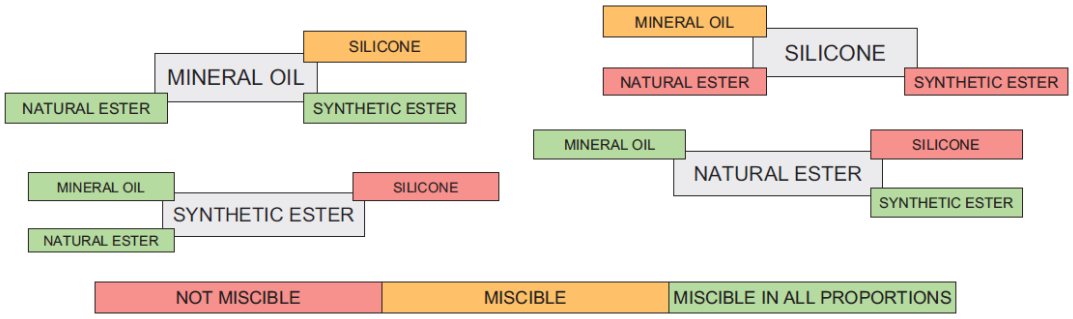

Figure 35. Miscibility of Alternative Fluids at Ambient Temperature.
(Source: Fernández et al., 2012)

Viscosity is known as the most important parameter for transformer cooling systems. All alternative fluids that has presented by Fernández et al. (2012) are more viscous than mineral oils. This is the critical point to determine the characteristics of cooling systems. In addition, moisture is absorbed by alternative fluids more than mineral oil. Moisture molecules are bounded on the winding insulation materials easily while using traditional transformer oils. Additionally, vegetable based transformer oils have tendency to absorb that moisture molecules contained within the insulation material. As a result, moisture in the insulation material is diminished and strengthens the aging withstand of insulation material. Therefore, using vegetable based transformer oils enables higher overloading capacity of transformers.

Rozga (2013) was presented a study on the properties of new environmentally friendly transformer oils for power transformers in 1st Annual International Interdisciplinary Conference. Basic properties of synthetic ester, natural ester and mineral oil were summarized as shown in Table 5. It is obviously shown that natural ester oil is more viscous than synthetic ester and mineral oil. Especially, at high temperatures, viscosity of natural ester is 3 times higher than the mineral oil. Fire resistance of transformer oils have significant role in safety regulations. Natural esters have very high fire and flash points as shown in table below. Also, the environmental impact of natural esters have drawn attention with 97% biodegradable value, while the synthetic ester and mineral oil have 89% and 10%, respectively. Due to environmental concerns, the future trend in transformer manufacturing is to increase the research on biodegradable and fire-proof transformer oils. At the moment, natural ester based transformer oils seems as the best option the industry have.

Table 5. Basic Properties of Synthetic Ester, Natural Ester and Mineral Oil.

Physico-chemical properties	**Units**	**Synthetic ester**	**Natural ester**	**Mineral**
Density at 20˚C	kg/dm³	0.97	0.92	0.88
Specific Heat at 20˚C	J/kgK	1880	1848	1860
Thermal Conductivity at 20˚C	W/mK	0.144	0.177	0.126
Kinematic Viscosity at 20˚C	mm²/s	70	85	22
Kinematic Viscosity at 100˚C	mm²/s	5.25	8.4	2.6
Pour Point	˚C	-60	-21	-50
Fire Point	˚C	316	360	170
Flash Point	˚C			150
Fire Hazard Classification to IEC 61100 / IEC 61039	-	K3	K2	0
Biodegradability	%	89	97	10

(Source: Rozga, 2013)

2.9. Overview of Thesis According to Literature

Determination of hot spot temperature in transformers is a challenge that has been studied by various researchers. The basic problems encountered in these studies are summarized below.

- The problem of determination of eddy currents in the windings requires 3D electromagnetic simulations as the transformers do not possess any symmetries. This is the electromagnetic part contribute to the phenomenon. This requires solution of Maxwell's equations in steady state and transient conditions.
- Determination of eddy currents is not enough to provide final solution to the identification of hot spot temperature. The problem is also dominated by thermal and fluid dynamic laws. This part of the problem brings great challenges as the transformer winding geometry is extremely complicated. Many parameters for instance winding type, spacer dimensions, disc dimensions, layer dimensions and cooling duct dimensions etc. further complicates the problem.
- Coupled electromagnetic and CFD solvers are readily available in the market today. However, in order to utilize these solvers, great simplifications in transformer CFD models are required. The basic simplification can be attained by finding ways to subtract the cooling systems from the geometry. This will enable the saving from both the mesh and the computation times.
- Geometry of the radiators is recently subject to changes as a result of new transformer oils introduced into the market. To provide new and deeper understanding related to these products requires new studies.

The abovementioned problems states that in order to provide complete coupled simulation of a power transformer requires simplifying cooling systems. Moreover, new radiator geometries and transformer oil performances has to be determined. In literature, the CFD models are generated by assuming constant flux densities where the fringing effects of electromagnetic flux lines are omitted. These studies also do not provide coupled simulations. Performance of new transformer oils has not been studied in detail.

Last but not least, modelling of transformer radiators with porous medium has not been encountered in literature in details. In these studies constant oil density was assumed and oil type and radiator geometry was not provided in detail. More importantly viscous and inertial resistance coefficients, the most important parameters in porous media approach, were not given apparently.

The work presented in this thesis provides an approximation to the performance verification and simplification of cooling systems to analyze a transformer. This thesis aims at providing guidance for complete coupled electromagnetic and CFD simulations. The work presented here provides the first and the fundamental step of complete coupled simulations. Hence, thermal and hydrodynamic characteristics of the transformer cooling systems will be provided by this study. Then, all the cooling systems of the transformer can be modelled as a porous medium in simulations to decrease the element number and computation time. CFD simulations and electromagnetic simulations should be generated to provide coupled solutions. All the simulation results should be also verified by experimental studies.

CHAPTER 3

TRANSFORMER OILS

Transformer oil is used in oil-filled transformers to provide electrical insulation and heat transfer, thus it is called as insulating oil. Transformer oils can be grouped into three main types in this thesis as shown in Figure 36: mineral, ester and silicone transformer oils. Ester based transformer oil is divided into two groups: natural ester and synthetic ester transformer oils. The most common type of transformer oil is mineral oil. Mineral oils negatively impact environment. Most importantly, it has poorly biodegradable (only 10%) as mentioned by Rozga (2013). Because of these reasons, it was decided that natural ester oil behavior in transformer should be investigated to collect more information for further developments. Also, dielectric properties of natural ester transformer oil are similar or better than mineral oil.

Figure 36. Transformer Oil Types.

Transformer oil analysis provides information regarding the transformer condition. It can be thought as a fingerprint of transformer. The properties of unused oil can be compared with the oil sample of transformer oil in service. A famous method to detect incipient falls is called dissolved gas analysis (DGA). Degradation of oil at cellulose insulation material generates certain gases. These gases are hydrogen, oxygen, carbon monoxide, carbon dioxide, ethylene and ethane etc. can be used to determine the type of fault and the cause of fault. A famous duval triangle method compares the volume of the generated gases and gives a description of the type of fault, fault temperature and the fault's origin as shown in Figure 37.

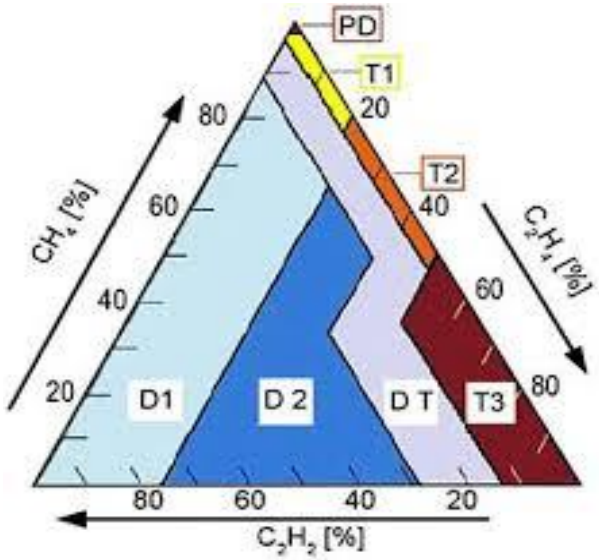

Figure 37. Duval Triangle.

(Source: Arora, 2013)

DGA also gives the trend of gases formation in the transformer oil leading to identify the type of fault. For instance, increase in percentage value of CH_4 while percentage of the other gases remain the same means that there is a high level of partial discharge (PD) on insulation materials. Another example can be demonstrated as C_2H_2 has 3% and C_2H_4 has 30% volume content. According to duval triangle mentioned by Arora (2013), the intersection of the lines lies in the area of T2 colored by orange. This means that the fault has a thermal fault with temperature 300 – 700 ˚C as shown in Table 6.

Table 6. Duval's Triangle Fault Zone.

Case	Fault Diagnosis	$\%CH_4$	$\%C_2H_2$	$\%C_2H_4$
PD	Partial Discharge	98%		
D1	Low energy discharge		> 13%	< 23%
D2	High energy discharge		%13 - %29	23% - 38%
			> 29%	> 23%
T1	Thermal fault < 300 deg C		< 4%	< 20%
T2	Thermal fault 300 - 700 deg C		< 4%	20% - 50%
T3	Thermal fault > 700 deg C		< 15%	> 50%
DT	Thermal & electrical fault	rest area		

(Source: Arora, 2013)

On line DGA analyze systems are integrated into modern transformers. These systems enable early detection of the faults prior to catastrophic failures. By monitoring the transformers in service enables users to identify possible fault types. This ensures that the manufacturer of the transformer can be responded to the fault before final failure. This explains the importance of transformer oil because transformer oil tests can be considered as finger print of transformer. It gives the health of transformer during its service life.

Furthermore, besides fault detection transformer oil serves as cooling and dielectric insulating medium. From heat transfer point of view, transformer oil enables to cool down the both the windings and the core through natural circulation. In order to increase the capacity of transformer further, pumps and fans can be added into cooling system. Cooling the transformer efficiently provides higher MVA ratings. 25 MVA natural circulating transformer can be increased up to 30 MVA just by adding cooling fans below the radiators. Therefore, efficient cooling increases transformer power rating as well as enables optimization in power transformer design.

In this study, flow and heat transfer of a transformer radiator filled with mineral oil, natural ester oil, synthetic ester oil and silicone oil were investigated. Density, specific heat, thermal conductivity and viscosity properties for the most common transformer oil types used in simulations were presented in this chapter. Also, the equations were obtained depending on the temperature for each property of each oil types to use it in Fluent while defining the material properties. All the graphs had drawn by using MathCAD.

Density, specific heat and thermal conductivity properties of the transformer oil are constructed using curve fitting techniques from the manufacturer's test data. These data are glugged into Fluent software by using piecewise-linear profile. Physical properties are defined at the 233 K and 383 K while using piecewise-linear profile. On the other hand, piecewise-polynomial profile is used to define viscosity. ANSYS Fluent software program uses the dynamic viscosity property. Therefore, dynamic viscosity graphs and equations were discussed in this study.

3.1. Density

As shown in Figure 38, density of the transformer oils decreases linearly with increase in temperature. Mineral transformer oil has the lowest density value, whereas the synthetic ester oil has the highest.

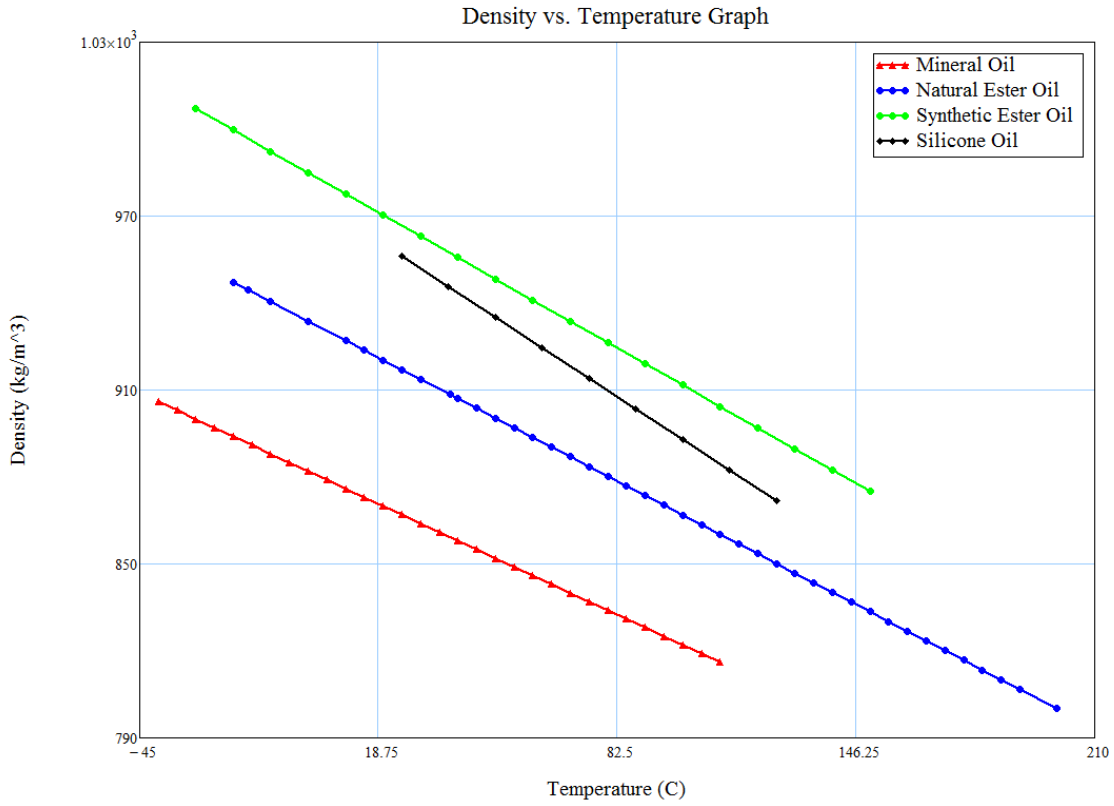

Figure 38. Density Graph versus Temperature.

3.2. Specific Heat

Specific heat is a kind of physical property of matter that defines the required heat to change a unit mass of a matter by one degree Celsius. As shown in Figure 39, specific heat values slightly increase with temperature. Specific heat versus temperature graph shows that the mineral oil has the highest specific heat values.

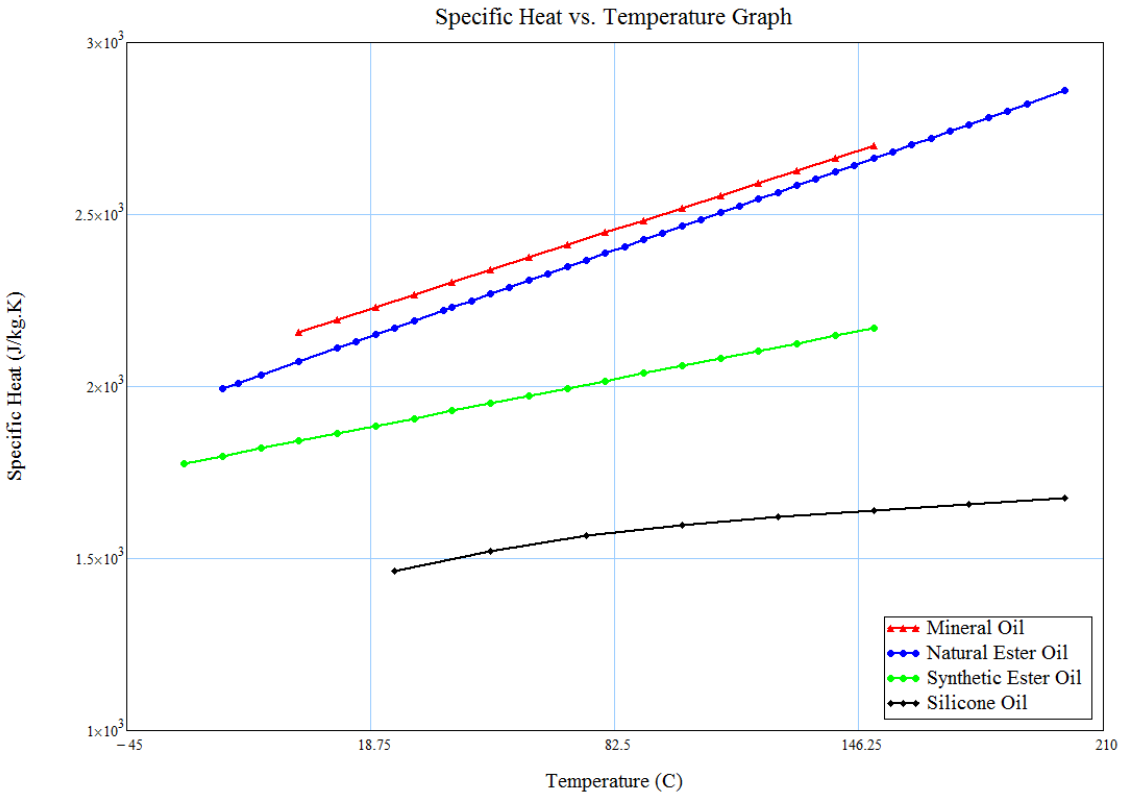

Figure 39. Specific Heat versus Temperature.

3.3. Thermal Conductivity

Thermal conductivity is a physical property of matter that related with conduction heat transfer. As shown below in Figure 40, thermal conductivity property of transformer oils linearly decreases with temperature. Silicone oil thermal conductivity value is constant, 0.151 W/mK. As a result, thermal conductivity versus temperature graph shows that natural ester oil and synthetic oil both have the same thermal conductivity values, whereas mineral oil has the lowest.

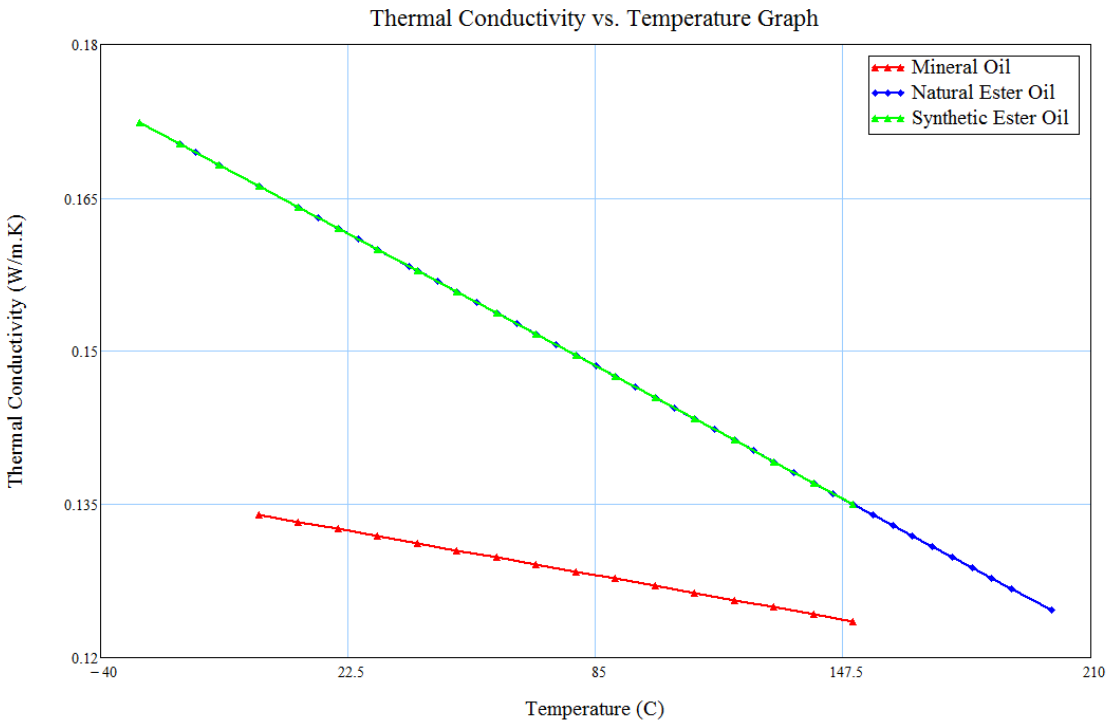

Figure 40. Thermal Conductivity versus Temperature.

3.4. Dynamic Viscosity

Although viscosity graphs were obtained exponential. Then the equations were defined in MathCAD using Levenberg – Marquardt non-linear method as shown in Equation 3.1.

$$\mu_{oil}(T) = e^{\left[C_i + \frac{C_{i+1}}{T+273.15} + C_{i+2}\cdot\left(\frac{1}{T+273.15}\right)^2 + C_{i+3}\cdot\left(\frac{1}{T+273.15}\right)^3 + C_{i+4}\cdot\left(\frac{1}{T+273.15}\right)^4\right]} \quad (3.1)$$

where c_i shows the coefficients that obtained from Levenberg – Marquardt non-linear method, T is the reference temperature and μ_{oil} is the dynamic viscosity of oil.

From dynamic viscosity versus temperature graph (Figure 41) it is clear that viscosity decreases with increasing temperature. Viscosity has the highest value at the low temperatures. There is a significant decrease in dynamic viscosity values between -20˚C and 0˚C.

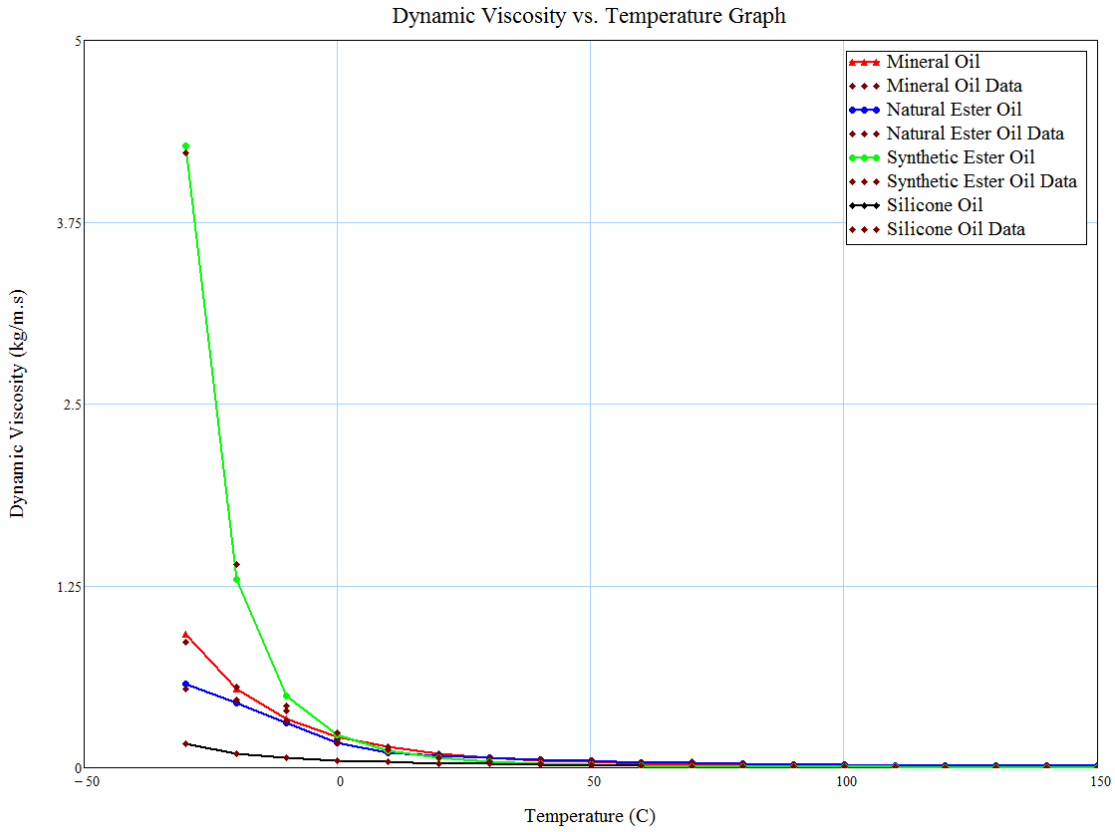

Figure 41. Dynamic Viscosity versus Temperature.

Although the viscosity equation was obtained, it is required that some special codes should be written to define exponential function in Fluent. Special codes that are known as user-defined functions (UDFs) allow the Fluent users to define special boundary conditions, material properties and source terms. However, it is required to have very well programming skills. Also, using UDFs could be complicated in some cases. Because of these reasons, viscosity graph was divided into two parts to have two different polynomial graphs. Equations of the each of viscosity graph were created by using curve fitting techniques in MathCAD. Then the coefficients were used in Fluent to define material property for each range by using piecewise-polynomial profile. First range was defined between 233 K and 303 K. Then, the second range was constructed between 303 K and 383 K. Detailed information about material properties was given in next chapter.

CHAPTER 4

NUMERICAL ANALYSIS

ANSYS Fluent is CFD simulation software to model fluid flow and heat transfer. This study illustrates the fluid flow and heat transfer problem in a section of transformer radiator. CFD simulation consists of four main parts as modelling, meshing, solution and results. ANSYS Fluent CFD solver uses finite volume method. Modelling and meshing works are specified as pre-processing and solution and results are defined as post-processing.

In this study, a section of a radiator was investigated. Methodologically, symmetry condition was used and quarter of the flow volume was created to investigate the fluid flow and heat transfer in radiator section.

Radiator geometry was modelled in Catia V5 software, and then imported into ANSYS Design Modeler module (Figure 42) to obtain a flow volume. Appropriate mesh elements were selected for each part.

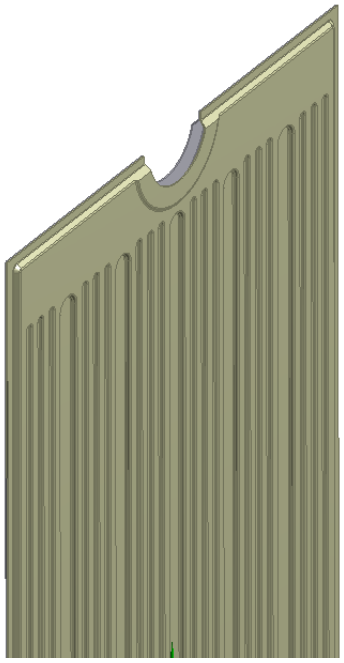

Figure 42. Imported Radiator Geometry in Design Modeler.

In setup module, temperature dependent material properties of transformer oil were defined. Boundary conditions and solution methods were selected. Results were obtained and visualized.

Computational fluid dynamics (CFD) calculations are based on three main equations; continuity, momentum and energy equations. The form of the continuity equation for laminar flow is shown in Equation (4.1). Steady-state flow regime was studied in this study. Fluid properties of the oil circulating through the radiator oil ducts do not change over time at any point. Partial derivatives of all quantities with respect to time are zero in steady-state flow regime. Radiator and directions are seen in Figure 43.

$$\frac{\partial(\rho u)}{\partial x}+\frac{\partial(\rho v)}{\partial y}+\frac{\partial(\rho w)}{\partial z}=0 \qquad (4.1)$$

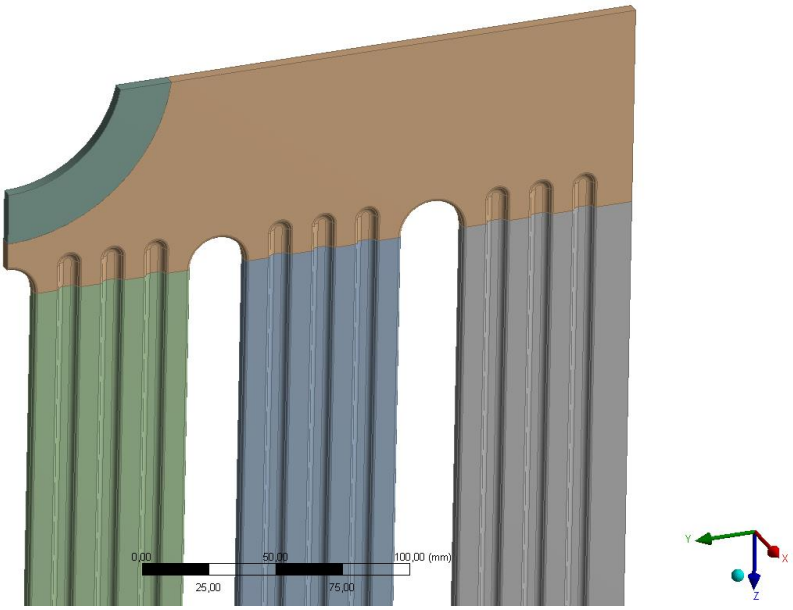

Figure 43. Radiator Model and Directions.

x, y, z-momentum equations are seen below in Equation (4.2)-(4.4), respectively.

x-momentum

$$\frac{\partial}{\partial x}(\rho uu)+\frac{\partial}{\partial y}(\rho vu)+\frac{\partial}{\partial z}(\rho wu)=-\frac{\partial P}{\partial x}+\mu\left[\frac{\partial^2 u}{\partial x^2}+\frac{\partial^2 u}{\partial y^2}+\frac{\partial^2 u}{\partial z^2}\right] \qquad (4.2)$$

y-momentum

$$\frac{\partial}{\partial x}(\rho uv) + \frac{\partial}{\partial y}(\rho vv) + \frac{\partial}{\partial z}(\rho wv) = -\frac{\partial P}{\partial y} + \mu\left[\frac{\partial^2 v}{\partial x^2} + \frac{\partial^2 v}{\partial y^2} + \frac{\partial^2 v}{\partial z^2}\right] \qquad (4.3)$$

z-momentum

$$\frac{\partial}{\partial x}(\rho uw) + \frac{\partial}{\partial y}(\rho vw) + \frac{\partial}{\partial z}(\rho ww) = -\frac{\partial P}{\partial x} - \rho g + \mu\left[\frac{\partial^2 w}{\partial x^2} + \frac{\partial^2 w}{\partial y^2} + \frac{\partial^2 w}{\partial z^2}\right] \qquad (4.4)$$

The energy equation of studied flow is as shown in Equation 4.5.

$$\rho c_p\left[\left(\vec{V}\cdot\nabla\right)T\right] = k\nabla^2 T + \left(\bar{\bar{\tau}}\cdot\nabla\right)\vec{V} \qquad (4.5)$$

4.1. Problem Statement

Simulation of power transformer requires a simplification of cooling systems because of mesh number and computation time. Porous model offers great amount of simplifications to the complete cooling system analysis. In order to quantify quarter of a single section of a radiator requires 2014258 element numbers. All the cooling system can be modelled as a single body by using porous medium approach. This enables extreme savings in terms of element number by this way. Therefore, one aim of this study is to enable complete transformer coupled electromagnetic and CFD model.

In order to achieve this modelling technique, single section of a transformer radiator is modelled and the pressure drop value is determined over a wide range of inlet velocity values at yearly average ambient temperature. Yearly average temperature is chosen because the transformer manufacturers design their system based on this temperature value.

Another important point of this study is to cover the thermal behavior of different and relatively new transformer oils. Their thermal properties are generated with MathCAD software to model these oil types in order to input these material properties into Fluent CFD Solver.

There are different transformer radiator manufacturers in the market. Every radiator manufacturer provides different solutions with different radiator geometries

before starting modelling phase one section radiator samples were provided from every manufacturer. Transformer radiator and oil ducts shapes are shown in Figure 44 below.

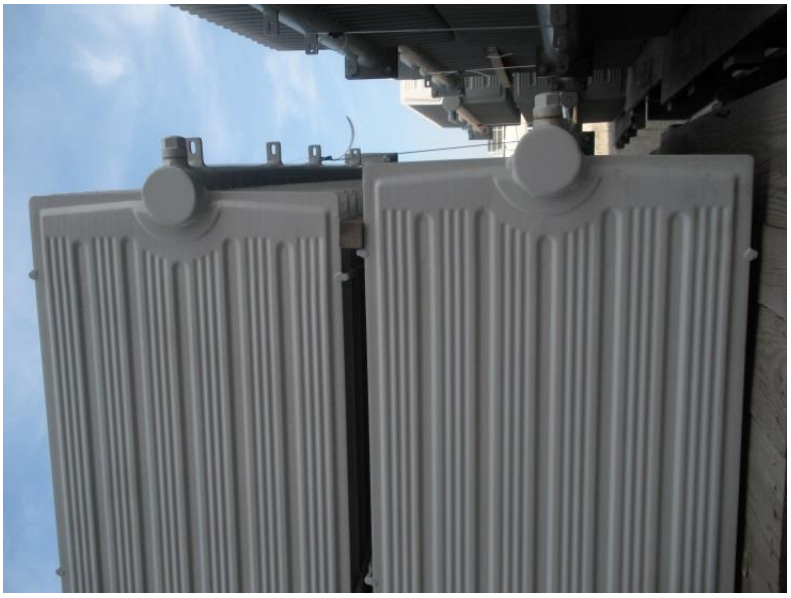

Figure 44. Transformer Radiator.

Radiators were cut with water jets to study and determine the oil duct geometries. Moreover, their cooling duct CAD geometries were obtained in order to compare actual geometry with the CAD geometries. No conflict between the CAD geometries and the actual geometries were found. Based on these studies actual modelling of one section transformer radiator was generated with ANSYS Design Modeler.

4.2. Modelling

Design Modeler is parametric geometry software that provides modelling features for ANSYS analysis. Transformer radiator geometry was modelled in CATIA V5 software as shown in Figure 45. The modelled radiator has the 3200 mm length and 520 mm wide. Geometry was imported into Design Modeler and modified to have a quarter of flow volume.

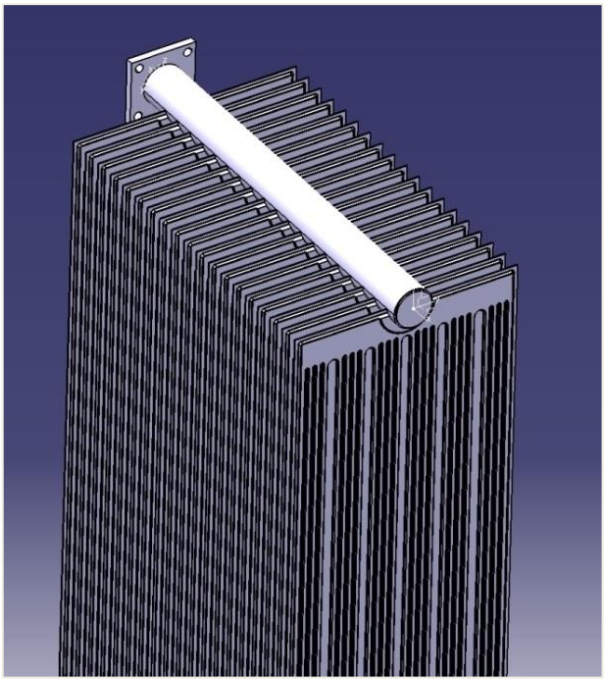

Figure 45. Radiator Model in Catia V5.

Radiator model was divided into parts according to grid element types. Inlet and outlet zones were simplified in this study as shown in Figure 46.

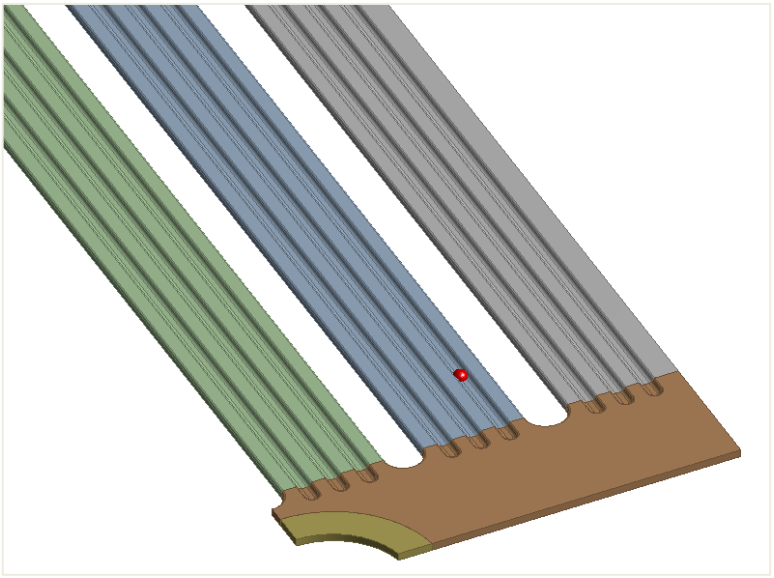

Figure 46. Simplified Radiator Model.

4.3. Meshing

Mesh (grid) module is the most important part of CFD simulations. In order to calculate the fluid flow and heat transfer of all body, domains are splitted into small parts, which are called mesh elements. ANSYS Fluent solver uses finite volume method to govern fluid flow and heat transfer equations. Boundary conditions should be defined before meshing operations.

In this study, inlet and outlet boundaries were defined as inlet-velocity and outlet-pressure, respectively. Symmetry boundary conditions were used by two symmetry planes to have a quarter flow volume.

Physical preferences were set to CFD and Fluent. Geometry was meshed by using different types of grid. Radiator oil ducts, inlet and outlet parts were meshed by using sweep mesh method with quad elements (Figure 47 and Figure 48). Quad meshes provide high quality solutions in sweepable bodies. Sweep mesh is a meshing method that has a high accuracy in CFD calculations. Inflation is defined to create thin elements near no-slip walls. Face zones were defined in boundary conditions. On the other hand, material properties influence the cells.

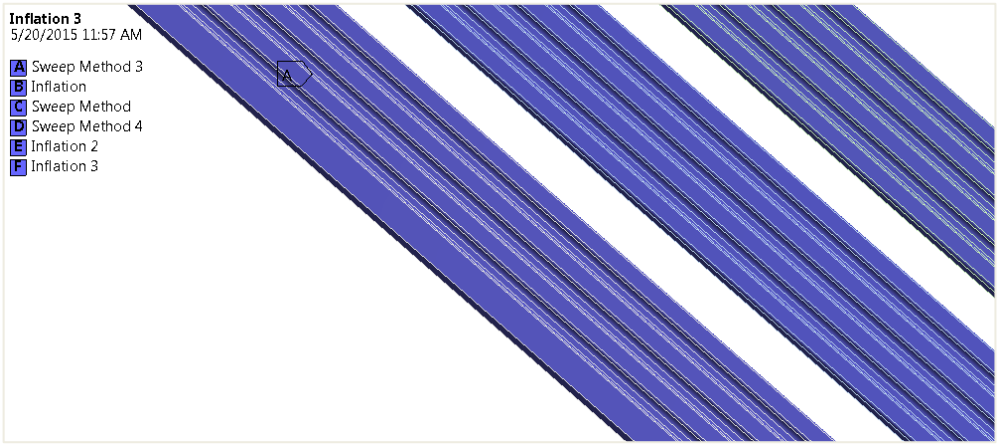

Figure 47. Mesh of the Oil Ducts.

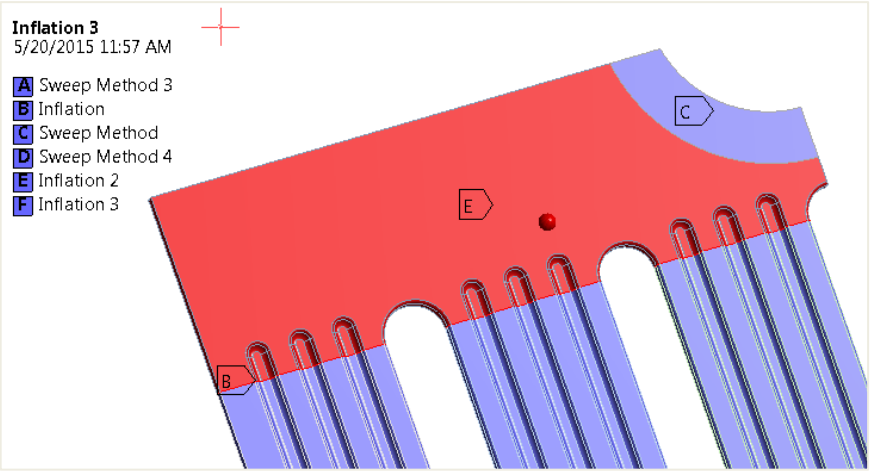

Figure 48. Inlet/Outlet Mesh Type and Inflation.

Inflation at the no-slip wall condition and quad mesh elements are shown in Figure 49.

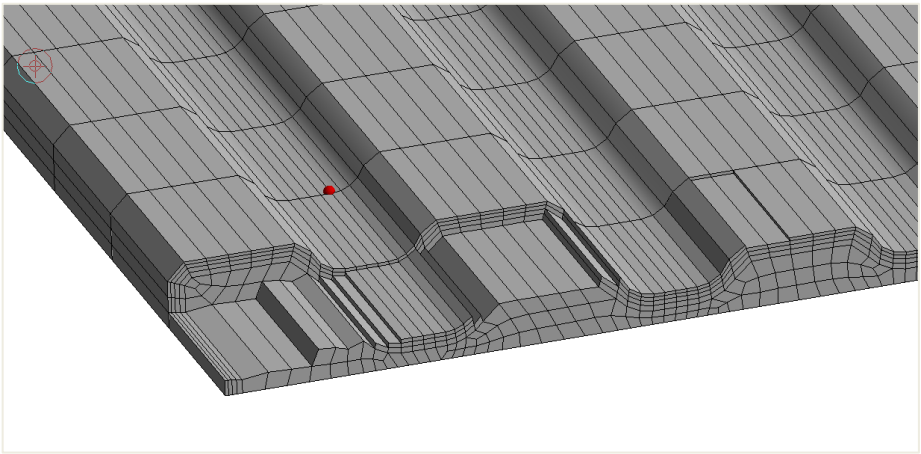

Figure 49. Section of Oil Duct.

Accuracy of the simulation is directly depends on the mesh quality. Skewness is an important parameter that shows the mesh quality. 2014258 mesh elements were used with 0.897 skewness as shown in Figure 50. Value of the skewness can be accepted up to 0.95.

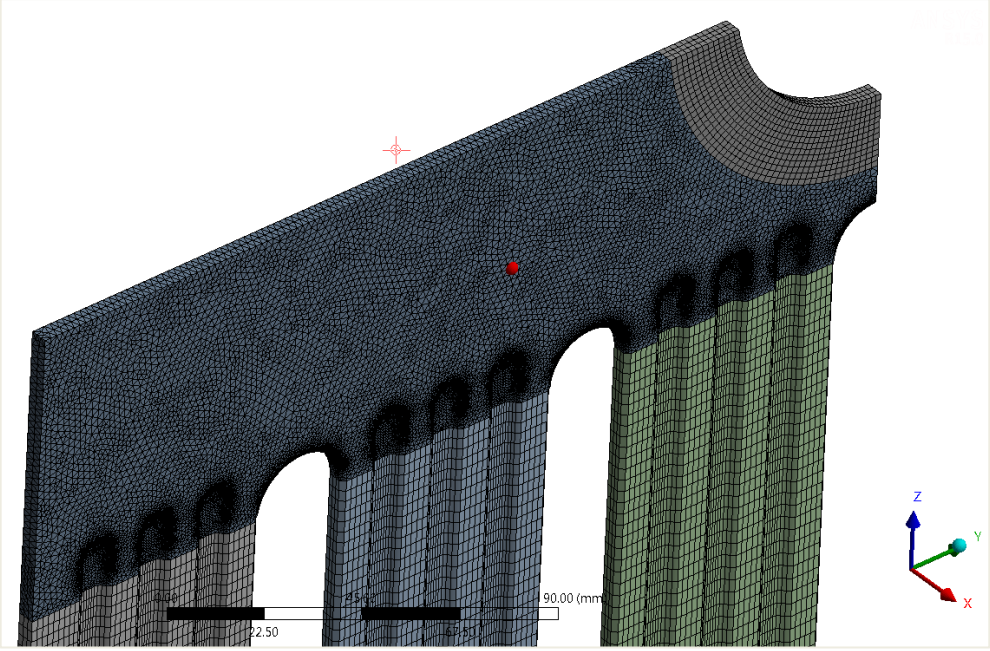

Figure 50. Mesh of the Radiator Model.

4.4. General Settings

Model settings, material properties, cell zone conditions, boundary conditions and reference values are the setup procedures. Solution methods, solution controls, monitors, initialization and calculations are performed in solution.

Pressure-based solver was used which is applicable for incompressible flow. Inlet and outlet area are equal and inlet velocity was defined constant. Therefore, mass flow rate at inlet and outlet are equal in each case. The velocity of transformer oil is independent of time at any point. Thus, steady-state flow regime was assumed in this study. Acceleration due to gravity was defined -9.81 m/s^2 along (-) z axis.

4.5. Viscous Model

The maximum thickness of oil duct is 9.1 mm as shown in Figure 51 and the height of the radiator is 3200 mm. Thickness of the oil duct is very small compared to the length of radiator. On the other hand, transformer oils have the high viscosity. Because of these conditions, flow is assumed as laminar.

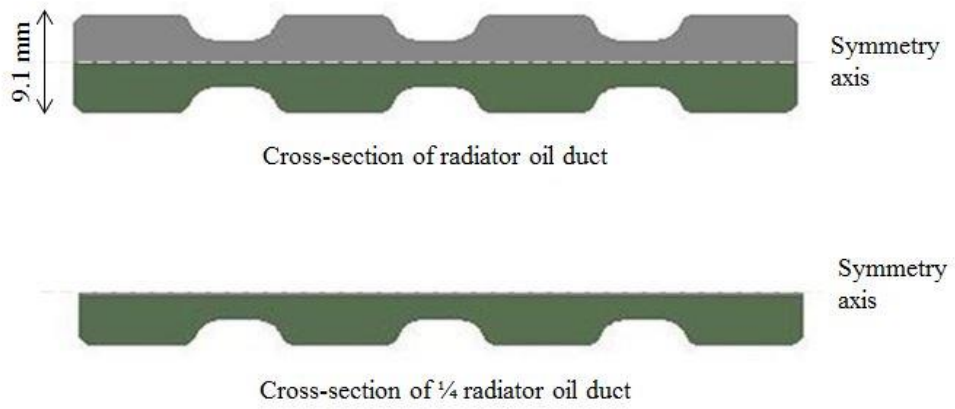

Figure 51. Cross-section of Radiator Oil Duct (top) and ¼ Radiator Oil Duct (bottom).

4.6. Material Properties

Temperature dependent material properties of transformer oil (density, specific heat, conductivity and viscosity) were defined in materials option.

Density of the transformer oils decrease linearly with increase in temperature, whereas the specific thermal capacity increases as shown in Chapter 3. Thermal conductivity also decreases with increasing temperature. Piecewise-linear method was used to define density, specific thermal capacity and thermal conductivity of transformer oils.

Viscosity graph is obtained exponential and its equation is defined in MathCAD using Levenberg – Marquardt non-linear method. However, special codes required to define this kind of complicated equations in Fluent. ANSYS Fluent allows defining undefined property with using user-defined functions (UDF). User needs programming skills to define UDF code.

In order to use UDF codes, piecewise-polynomial method in Fluent is used to define viscosity property. Viscosity graphs are divided into two parts and the equations are obtained for each part. Divided viscosity graphs are shown below. Fourth degree polynomial equation was obtained for natural ester transformer oil viscosity as shown in Equation (4.6) and Equation (4.7).

$$\mu(T) = 0.000000000081T^4 - 0.00000014036T^3 + 0.000091453076T^2 - 0.0265799317713T + 2.9142493540421 \quad (4.6)$$

$$\mu(T) = 0.0000000245382T^4 - 0.0000312372486T^3 + 0.0149171842259T^2 - 3.1680682038423T + 252.5684734582901 \quad (4.7)$$

Obtained polynomial equations and dynamic viscosity values for natural ester transformer oil are seen in Figure 52 and Figure 53. First interval of graph is defined from 253 K to 333 K, and second interval is from 333 K to 473 K. Red points indicates the measured viscosity values that are given and blue lines shows the equation results.

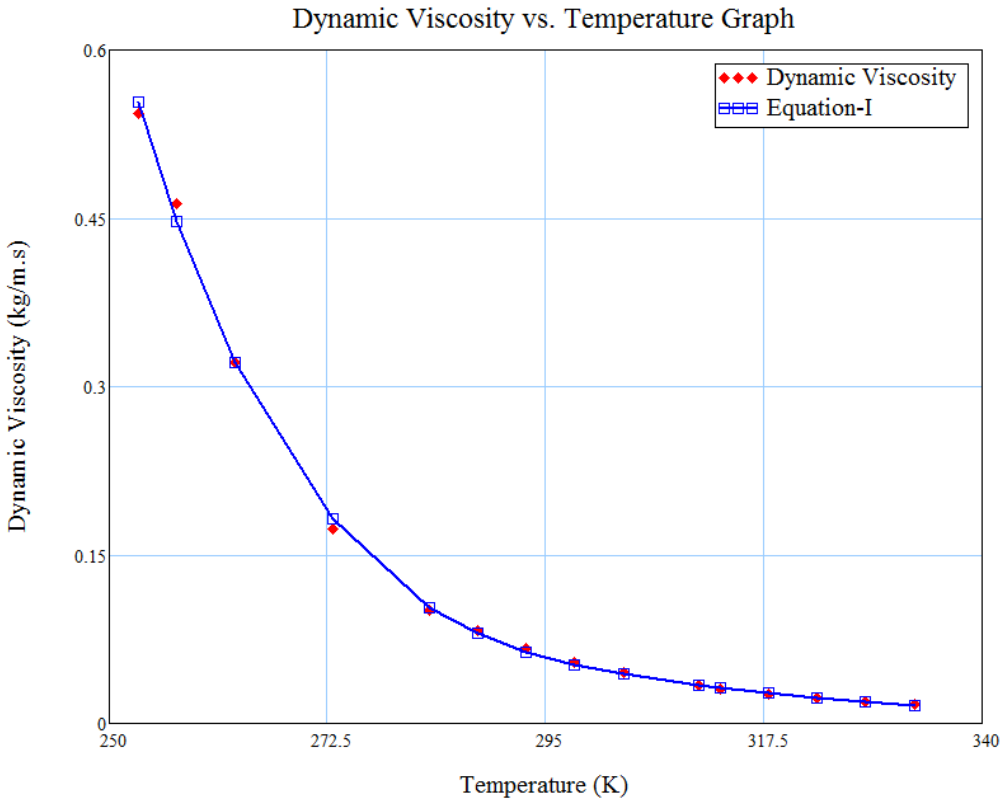

Figure 52. Dynamic Viscosity versus Temperature Graph of the First Interval for Natural Ester Transformer Oil.

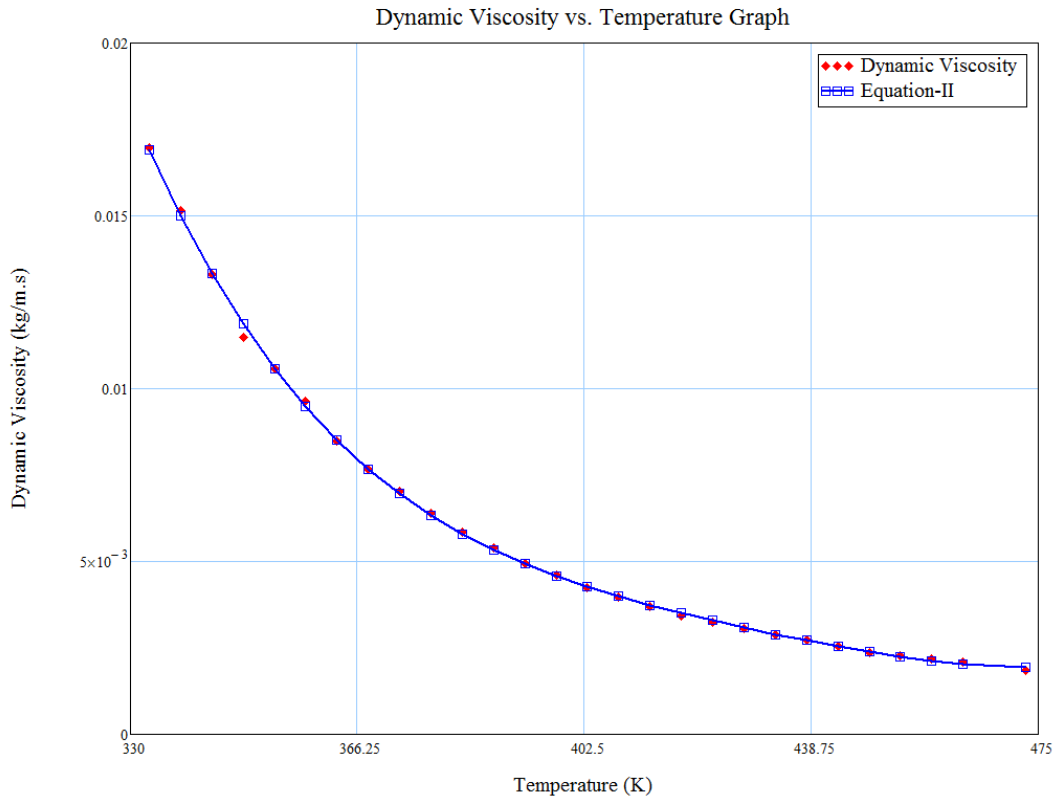

Figure 53. Dynamic Viscosity versus Temperature Graph of the Second Interval for Natural Ester Transformer Oil.

Moreover, material properties of radiator steel were selected constant. Density, specific heat and thermal conductivity of radiator steel were 7850 kg/m^3, 490 J/kg K, 46 W/m K, respectively.

4.7. Boundary Conditions

Inlet velocity, outlet pressure and symmetry boundary conditions are defined as shown in Figure 54.

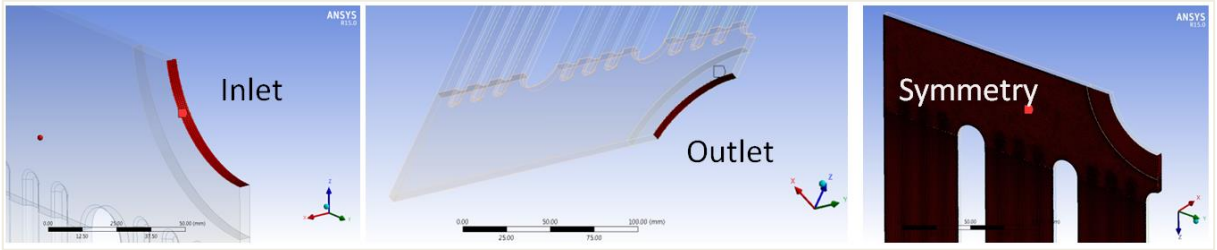

Figure 54. Boundary Conditions.

Inlet velocity and temperature conditions were defined based on the following principle. In transformers, various numbers of radiators are placed side by side. According to the measurements that has been carried out in Balikesir Electromechanical Industrial Plants Corporation Test Laboratories (Figure 55) the following velocity profiles for ONAN cooling mode was measured. The average oil flow velocity of 20 radiators placed side by side was found to range between 0.01 m/s to 0.035 m/s based on the loading and ambient temperature conditions. Ambient temperature at these measurements was 20˚C. This temperature value corresponds to 80˚C top oil temperature.

Figure 55. BEST Co. Test Laboratory.

In the simulations, the values for velocity and ambient temperature are taken into account based on these considerations. Moreover, in IEC 60076-2 Standard yearly average ambient temperature for transformer design is also given as 20˚C. Therefore, velocity profile at this temperature correspond both the standards and the measurements.

The aim of the study is to determine pressure drop, outlet temperature and heat flux of a transformer radiator based on different velocity values. For instance, overloading of transformer generates more heat and this might change the velocity

value at the inlet. In order to cover this difference and to determine the radiator pressure drop values for a wider range of velocities simulations were extended to cover 0.05 m/s.

0.01 to 0.05 m/s velocities and 353 K temperature were defined in velocity inlet boundary condition.

Outlet pressure boundary condition was defined to investigate the flow and heat transfer at outlet. Then, other surfaces were defined as wall automatically by Fluent. Heat transfer coefficient, free stream temperature, wall thickness and material settings were identified in wall settings. Thermal heat transfer coefficient was assumed as 6 W/m^2K in this study. Ambient temperature was 298 K.

4.8. Solution

Steady-state problem was investigated in this study, SIMPLE (Semi-Implicit Method for Pressure-Linked Equations) algorithm was selected in solution methods. Velocity and pressure gradients were calculated to solve momentum equation. Then pressure field was calculated by using under-relaxation factor for pressure.

Firstly, only the flow was investigated by closing the energy equations under Solution Controls menu to simplify iterations. After converged flow simulation, energy equation was opened.

Iteration results were observed by adding required variable into Surface Monitors. In this study, inlet pressure, outlet pressure, outlet temperature, inlet density, outlet density and heat flux at wall were defined in Surface Monitors. Variables were reported by using area-weighted average report type.

Before starting calculations, solution is initialized using standard initialization. Iterations continue and the monitors were followed until the solution converges. As seen in Figure 56, solution was converged after nearly 1200 iterations. Convergence criteria were 10^{-4} for the continuity and momentum equations and 10^{-9} for energy equation.

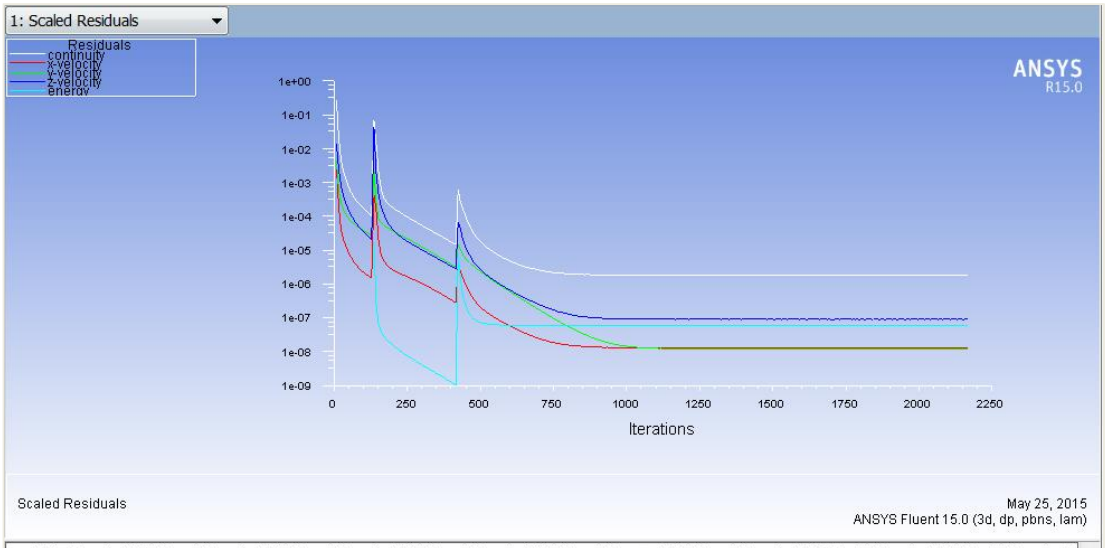

2157	1.8536e-06	1.3136e-08	1.2203e-08	9.1922e-08	5.8668e-08	1.9077e+02	0.0000e+00	3.4
2158	1.8619e-06	1.3229e-08	1.2285e-08	9.2464e-08	5.8423e-08	1.9077e+02	0.0000e+00	3.4
2159	1.8477e-06	1.3159e-08	1.2233e-08	9.1637e-08	5.8293e-08	1.9077e+02	0.0000e+00	3.4
2160	1.8546e-06	1.3128e-08	1.2217e-08	9.1605e-08	5.8083e-08	1.9077e+02	0.0000e+00	3.4
iter	continuity	x-velocity	y-velocity	z-velocity	energy	in-press	out-press	o
2161	1.8441e-06	1.3107e-08	1.2220e-08	9.1006e-08	5.7961e-08	1.9077e+02	0.0000e+00	3.4
2162	1.8572e-06	1.3146e-08	1.2224e-08	9.2114e-08	5.8124e-08	1.9077e+02	0.0000e+00	3.4

Figure 56. Scaled Residuals.

CHAPTER 5

RESULTS AND DISCUSSION

ANSYS Fluent CFD simulations use finite volume method to solve continuity, momentum and energy equations. CFD flow volume was created to simulate transformer oil flow in radiator.

Fluid flows are classified into two groups as compressible and incompressible flows. Incompressibility is a fluid dynamics property that describes the flow. In this study, incompressible flow was studied. Incompressible flows have small changes in density. Liquids are generally classified as incompressible fluids. Velocity inlet is a boundary condition in ANSYS Fluent CFD software. Velocity inlet boundary condition was used at inlet with constant velocity. Different velocity values were applied at this boundary. Also, inlet temperature was specified as 353 K for all simulations. Convection heat transfer thermal condition was defined at wall. Then, heat transfer coefficient was assumed as 6 W/m^2K. Thermal heat transfer coefficient characteristics on radiator inner and outer surfaces should be studied in the future works.

Flow was assumed as uniform at inlet. Additionally, symmetry boundary conditions were used to reduce computational domain. On the other hand, radiator boundary condition was not used for this problem. Because pressure drop and heat transfer coefficient characteristics does not known. One of the most important purpose of this study is to determine the characteristics of radiators that can be used in future works.

The most important limitation of the study is the mesh procedure. Researchers prefer the Catia or Inventor to design geometry instead of ANSYS Design Modeler module. Then, geometry should be updated in Design Modeler and also in Mesh module to avoid creating sharp edges. High performance computers are required to perform the calculations in 3D CFD simulations.

5.1. CFD Results

Results module is the CFD post-processing module in ANSYS software to visualize the flow and heat transfer in the simulation model. In this section, natural ester transformer oil will be investigated with visualizing temperature distribution, velocity vectors, heat flux and velocity streamlines of one quarter of transformer radiator section. According to the results, geometry of transformer radiators can be improved. Especially, at the corners heat transfer rate is lowest. Sharp corners can be rounded. Moreover, Reynolds number, Nusselt number and Prandtl number were calculated theoretically.

5.1.1. Temperature Distribution

Inlet temperature was set to 353 K at inlet boundary for all numerical analysis. The detailed temperature distributions around inlet and outlet zones are seen in Figure 57 and Figure 58. According to legend, red zone is around 353 K and blue zone is around 332 K. Also, temperature distribution along the simulated quarter model is seen in Figure 59.

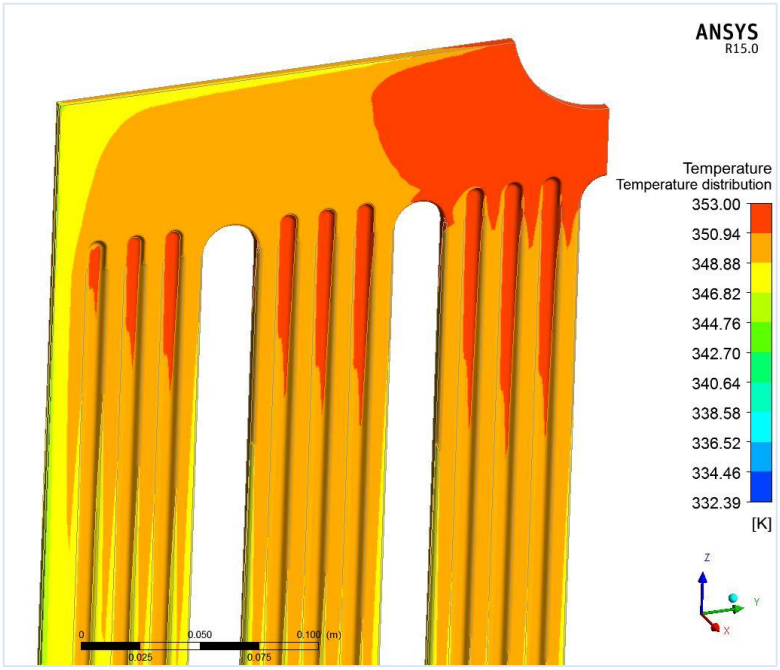

Figure 57. Temperature Distribution at the Inlet Zone with 0.05 m/s Inlet Velocity for Natural Ester Oil.

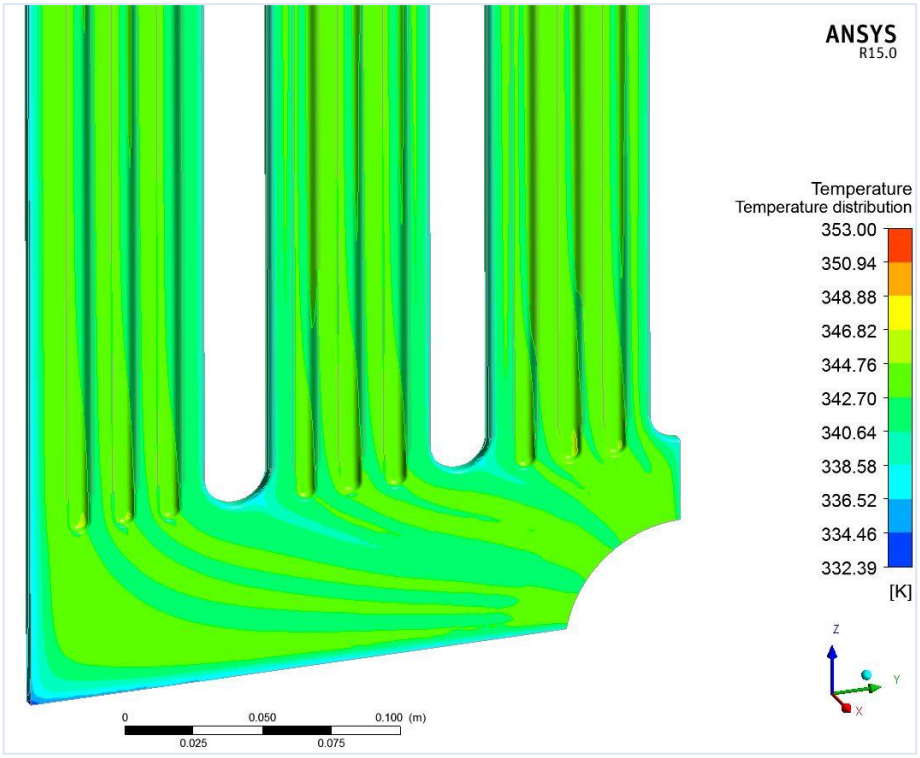

Figure 58. Temperature Distribution at the Outlet Zone with 0.05 m/s Inlet Velocity for Natural Ester Oil.

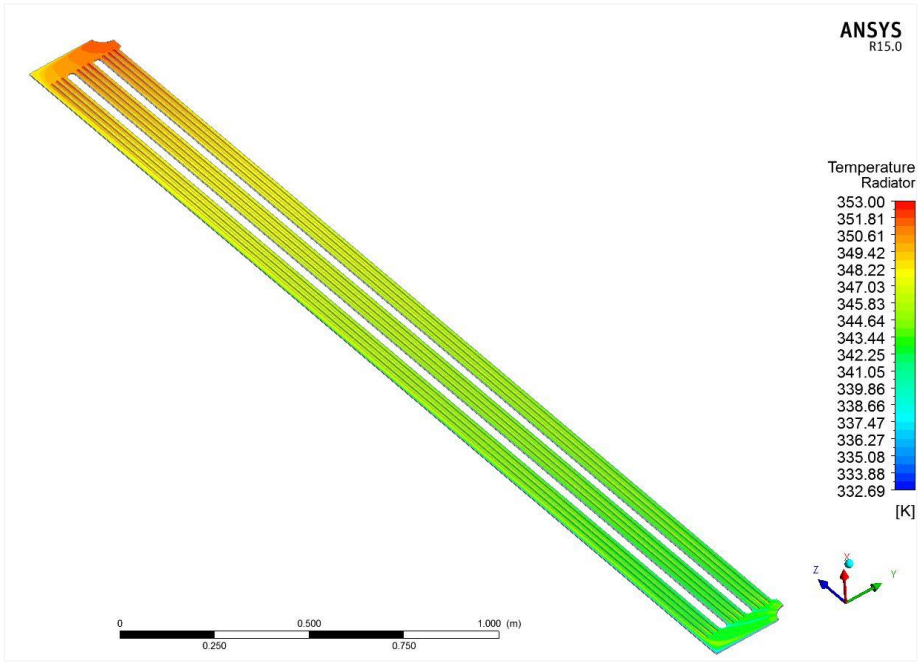

Figure 59. Temperature Distribution Along Simulated Quarter Radiator.

5.1.2. Velocity Vectors

Additionally, velocity profile of natural ester transformer oil was investigated that has 0.05 m/s at inlet. Velocity vectors were defined as normal to boundary to avoid the reversed flows at outlet boundary as seen in Figure 60 and Figure 61.

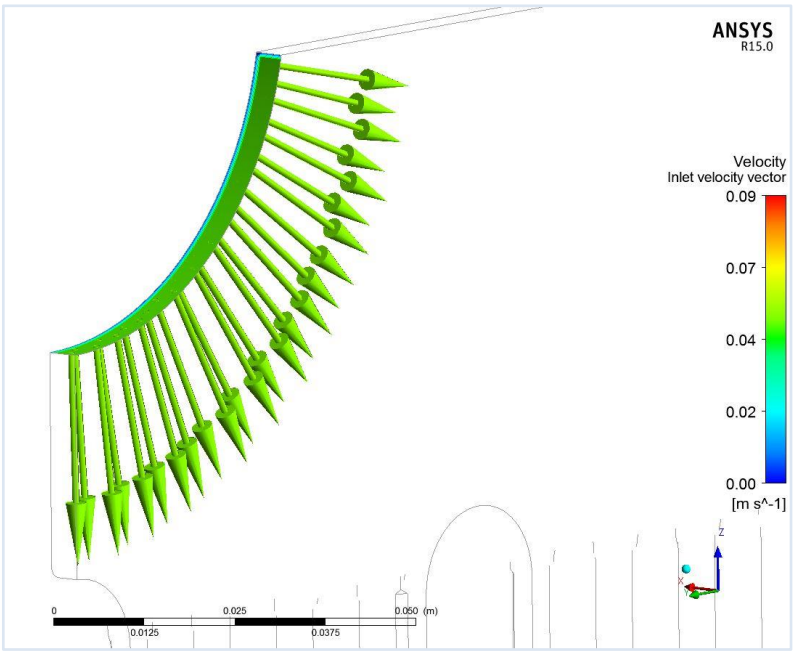

Figure 60. Velocity vectors at the inlet with constant 0.05 m/s inlet velocity.

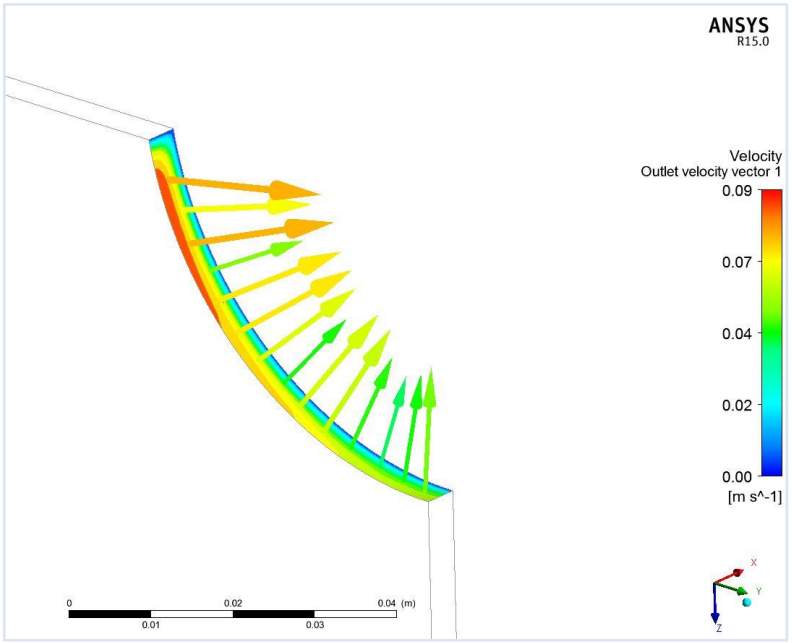

Figure 61. Velocity Vectors at the Outlet with Constant 0.05 m/s Inlet Velocity.

5.1.3. Velocity Streamlines

Streamlines were sketched for this flow to create velocity profile. Although the inlet velocity was 0.05 m/s, it is seen that velocity is decreased to nearly zero inside the oil ducts as shown in Figure 62. This velocity decreasing because of the small thickness that oil ducts have. Especially, at low temperatures natural transformer oil cannot flow inside the radiator with this traditional method. Velocity streamlines at inlet and outlet zones were shown in Figure 63 and Figure 64, respectively.

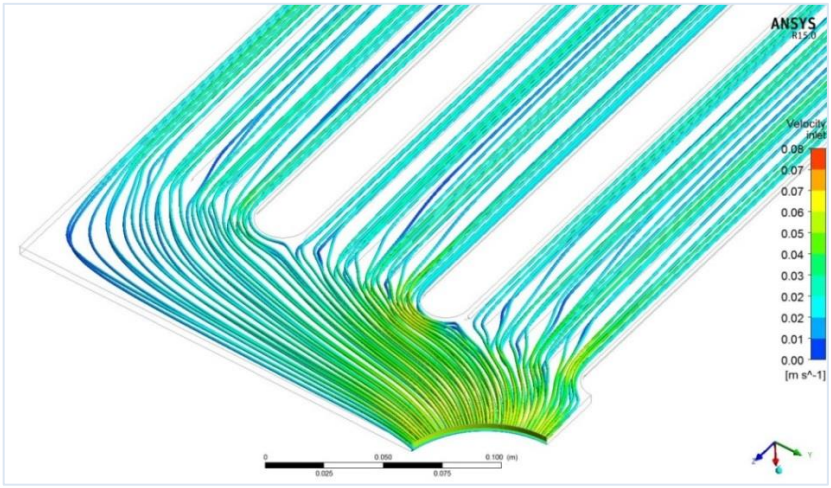

Figure 62. Streamlines at Inlet of Natural Transformer Oil with 0.05 m/s.

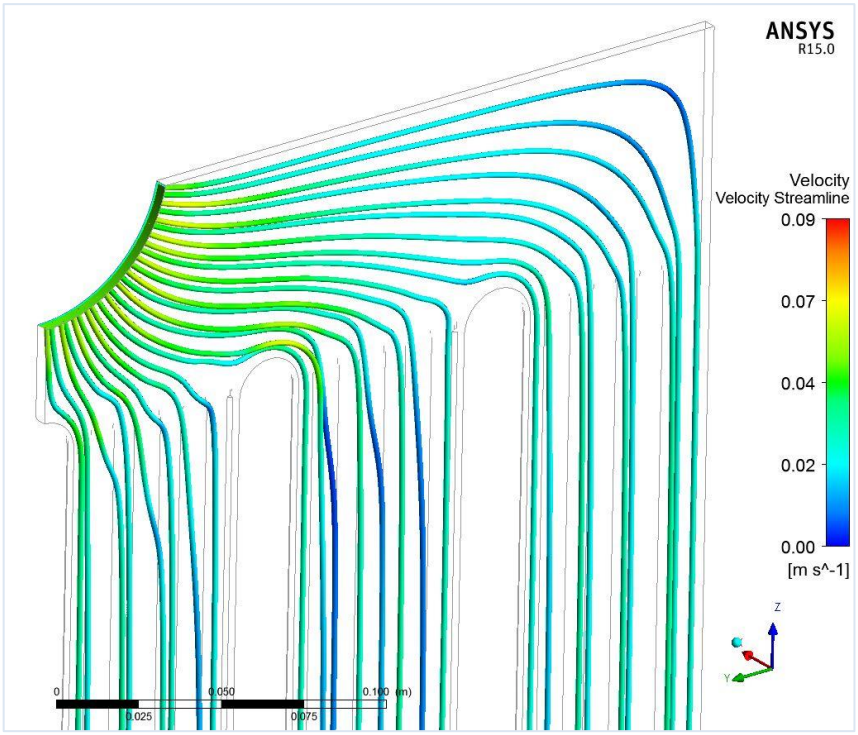

Figure 63. Velocity Streamline with 0.05 m/s Inlet Velocity at Inlet Boundary Condition for Natural Ester Transformer Oil.

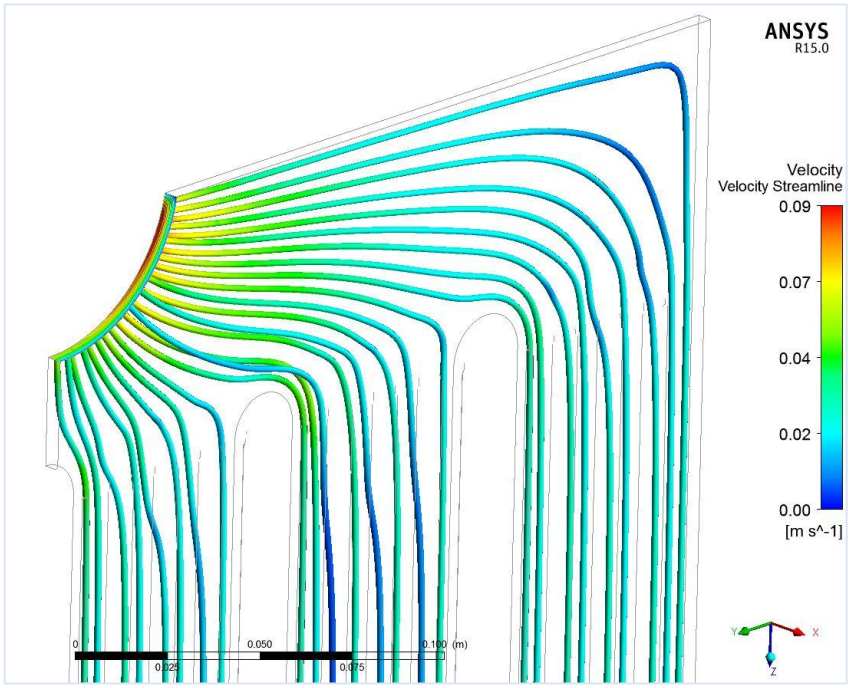

Figure 64. Velocity Streamline with 0.05 m/s Inlet Velocity at Outlet Boundary Condition for Natural Ester Transformer Oil.

The flow furthest from the inlet region in y direction can be accelerated by introducing an appropriate gap in the entry zone as shown in Figure 65. The grey shaded zone in Figure 65 will decrease the cross-sectional area and hence the velocity of streamlines along y direction will increase. This will increase the efficiency of the transformer radiators and suggested as an improvement based on the outcomes of this study.

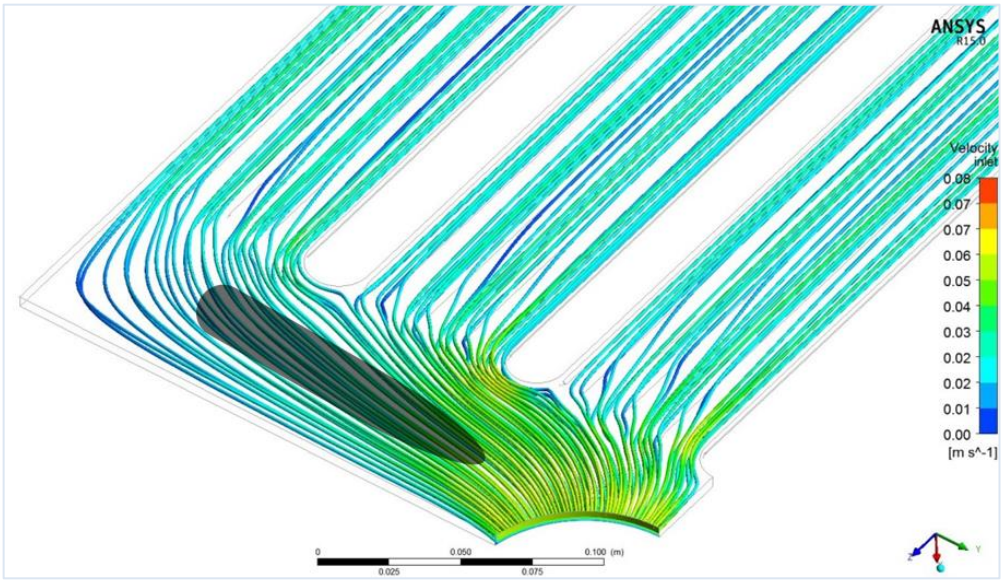

Figure 65. Recommended radiator entry zone.

5.1.4. Heat Flux

Heat flux at inlet zone and outlet zone were visualized by using 0.05 m/s velocity for natural ester transformer oil as shown in Figure 66 and Figure 67, respectively. Average heat flux is 284.9 W/m^2. Heat flux on radiator surface was shown in Figure 68.

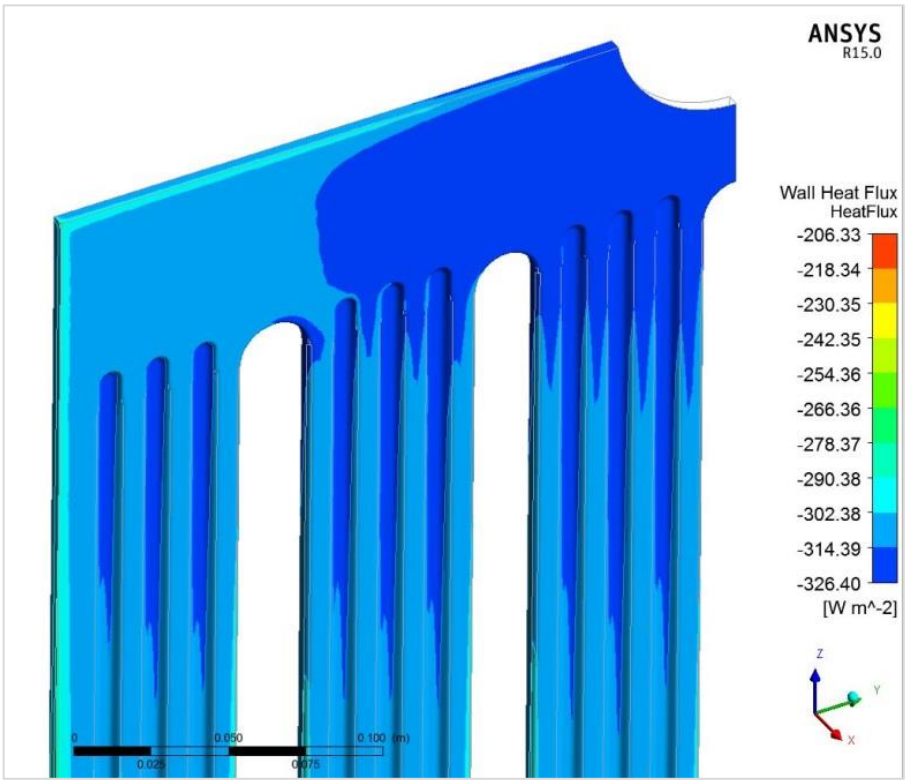

Figure 66. Heat Flux at the Inlet Zone with 0.05 m/s Inlet Velocity for Natural Ester Transformer Oil.

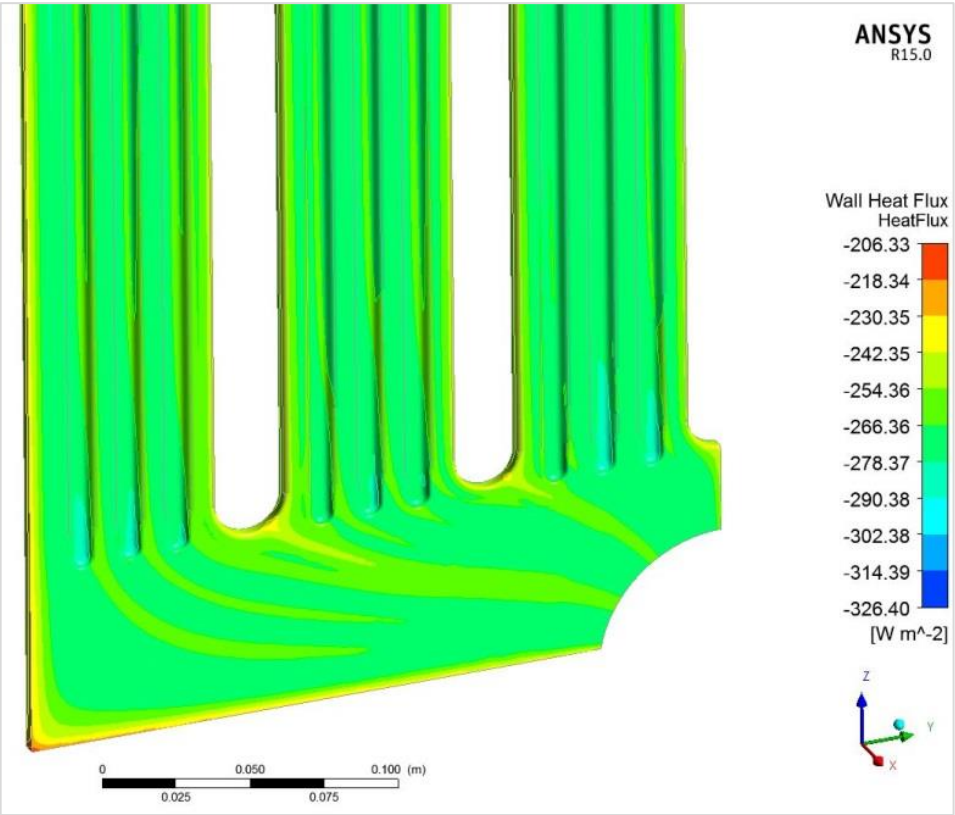

Figure 67. Heat Flux at the Inlet Zone with 0.05 m/s Inlet Velocity for Natural Ester Transformer Oil.

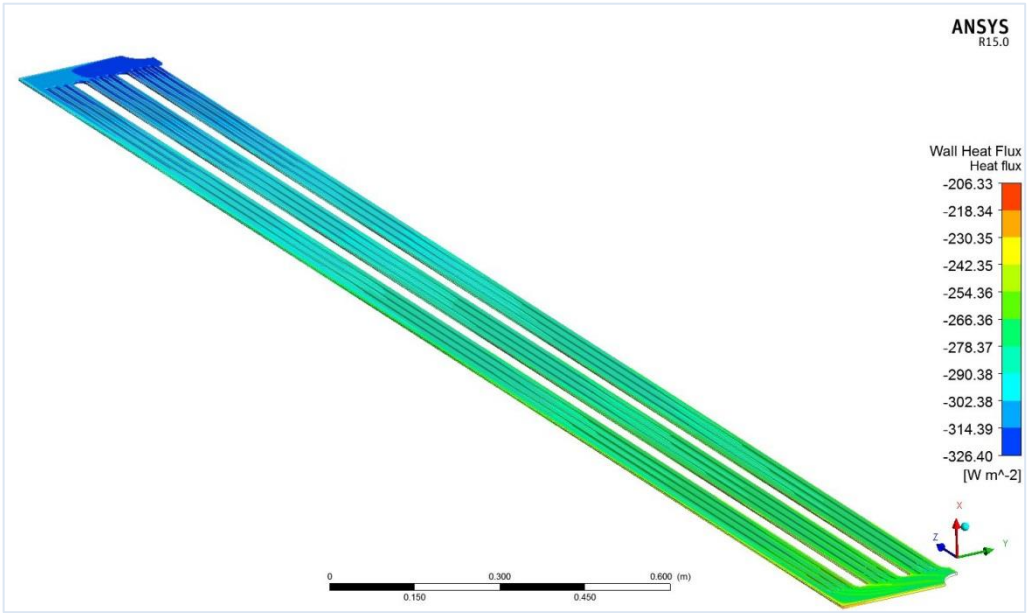

Figure 68. Heat Flux with 0.05 m/s Inlet Velocity for Natural Ester Oil.

5.1.5. Comparison of Oils

As shown in Table 7 and Table 8, the outlet temperature of radiators is the same which were simulated with natural ester and mineral transformer oil, respectively. Besides that, heat flux of each simulated radiator is the same. On the other hand, pressure difference between inlet and outlet of the radiator simulated with natural ester transformer oil is more than mineral oil. Silicone transformer oil has the most pressure drop as shown in Table 9. Although mineral oil has the lowest pressure drop and the highest heat flux, they should be replaced by natural ester transformer oils according to environmental concerns. Pressure difference increases by increasing the inlet velocity and heat flux also increases. Besides, temperature difference between inlet and outlet is decreasing by increasing velocity. Transformer oil temperature should be kept in working temperature limits. Because of that, minimum temperature difference and maximum heat flux is preferred in transformer cooling. The most heat flux with minimum temperature difference was observed in natural ester transformer oil as shown in Table 7. Additionally, temperature difference between the inlet and outlet of transformer winding has to be kept as low as possible according to Kim et al. (1987). The difference between inlet and outlet temperature of the transformer winding can be kept minimum, if mass flow rate of radiator can be increased. This can be achieved by increasing value of pressure drop along a closed circulating loop.

Table 7. Natural Ester Transformer Oil Results.

Velocity	**Pressure Difference**	**Heat flux**	**Outlet Temperature**	**Temperature Difference (inlet-outlet)**
[*m/s*]	[*Pa*]	[W/m^2]	[*K*]	[*K*]
0.02	94.9	258.7	337.1	15.9
0.03	127.5	272.6	341.7	11.3
0.04	159.3	280.1	344.1	8.9
0.05	190.8	284.9	345.7	7.4

Table 8. Mineral Transformer Oil Results.

Velocity	**Pressure Difference**	**Heat flux**	**Outlet Temperature**	**Temperature Difference (inlet-outlet)**
[*m/s*]	[*Pa*]	[W/m^2]	[*K*]	[*K*]
0.02	37.2	258.4	337.0	16.1
0.03	47.0	272.0	341.6	11.4
0.04	56.0	279.2	344.1	8.9
0.05	64.6	283.7	345.7	7.3

Table 9. Silicone Transformer Oil Results.

Velocity	**Pressure Difference**	**Heat flux**	**Outlet Temperature**	**Temperature Difference (inlet-outlet)**
[*m/s*]	[*Pa*]	[W/m^2]	[*K*]	[*K*]
0.02	151.8	240.6	331.7	21.3
0.03	206.6	259.2	337.6	15.4
0.04	260.0	269.3	340.8	12.2
0.05	312.9	275.8	343.0	10.1

Table 10. Synthetic Transformer Oil Results.

Velocity	**Pressure Difference**	**Heat flux**	**Outlet Temperature**	**Temperature Difference (inlet-outlet)**
[*m/s*]	[*Pa*]	[W/m^2]	[*K*]	[*K*]
0.02	80.4	253.5	335.7	17.3
0.03	103.9	268.4	340.6	12.4
0.04	126.5	276.5	343.3	9.7
0.05	148.7	281.5	345.0	8.0

The flow of an incompressible Newtonian fluid was studied. The thickness of radiator is very small compared to length. Therefore, fluid flow was defined as laminar

as in the case of a real transformer radiator flow. Additionally, thermal properties of oil and low velocity affect the flow regime.

Velocity versus pressure difference graph was drawn for each oil types as shown in Figure 69. It is seen that pressure difference is approximately the same for natural ester and synthetic oil. Mineral oil has the minimum pressure difference and silicone oil has the highest.

As shown in Figure 70, natural ester oil has the maximum heat transfer rate and it is nearly same as mineral oil. The lowest heat transfer rate is seen for silicone oil. Also, heat transfer increases with velocity of transformer oil.

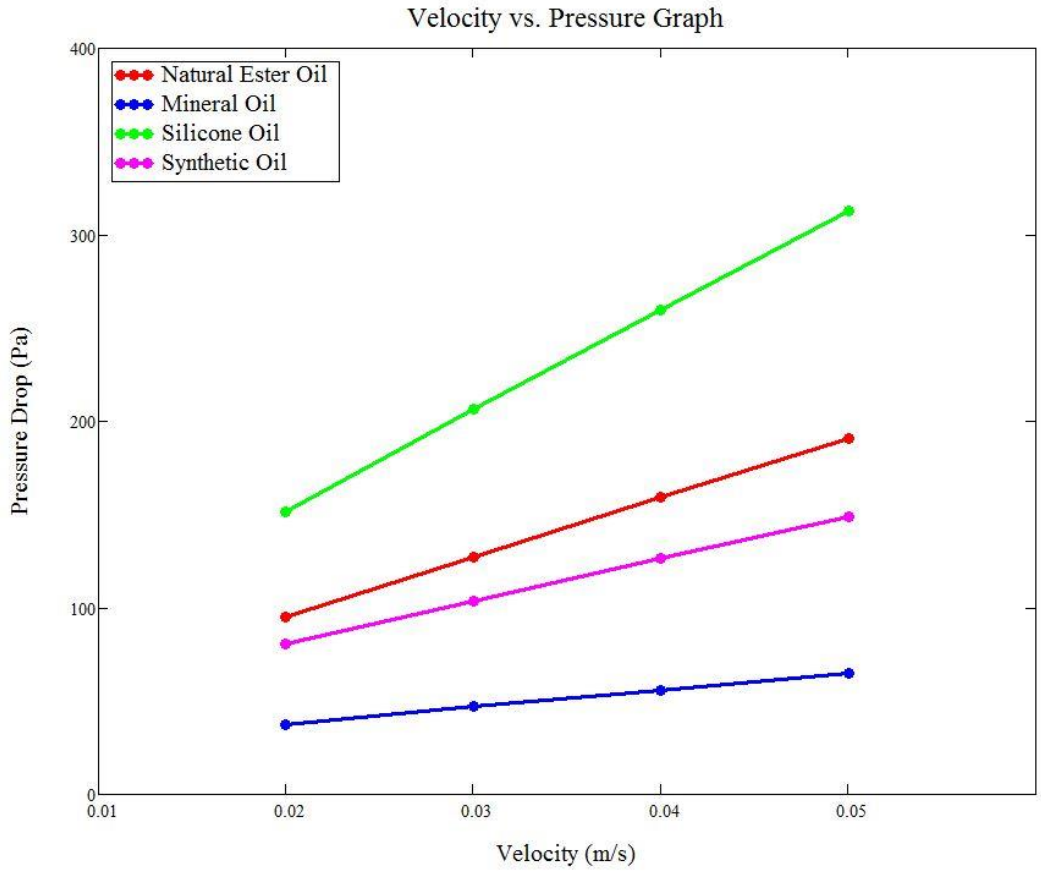

Figure 69. Velocity versus Pressure Drop Graph.

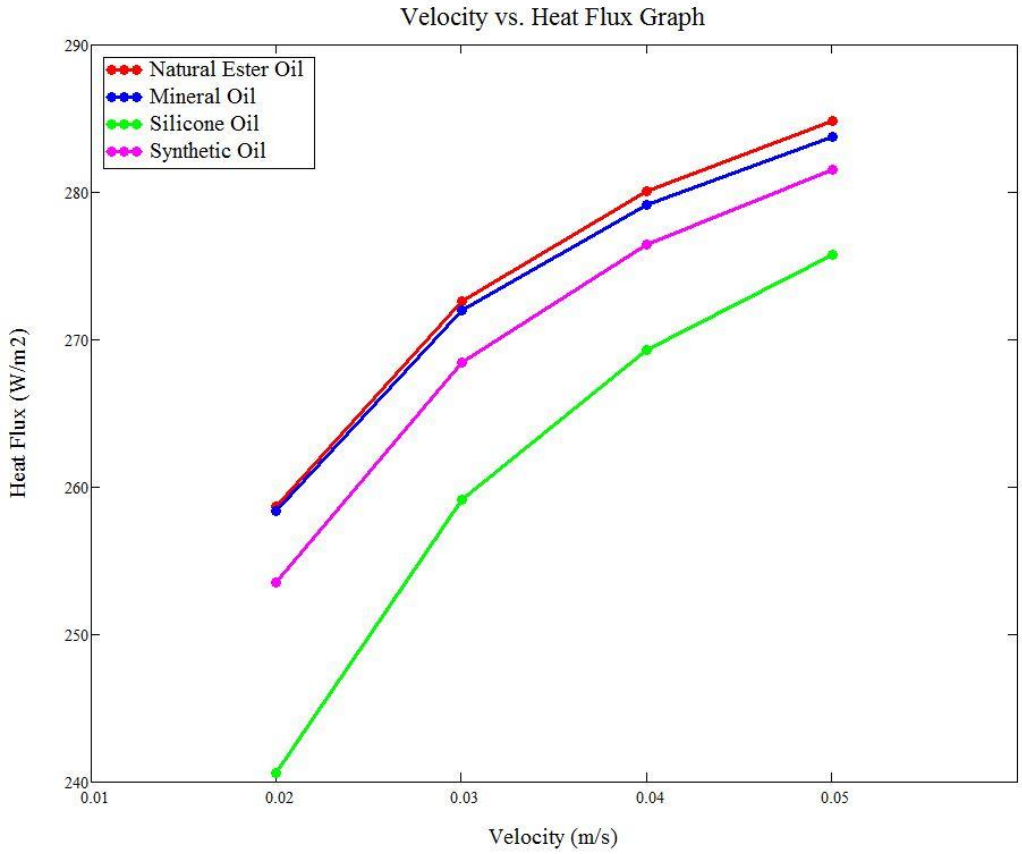

Figure 70. Velocity versus Heat Flux Graph.

5.1.6. Dimensionless Numbers

This section includes the dimensionless number of flow in radiator with natural ester transformer oil. As mentioned last section, natural ester transformer oil has the best heat flux. Natural ester transformer oil was investigated in this section.

Reynolds numbers of natural ester transformer oil flow were calculated for each case as shown in Table 11. Reynolds number is a dimensionless number in fluid mechanics that defines the flow regime. Ratio of inertial forces to viscous forces gives the Reynold number as shown in Equation (5.1), where ρ is the average density of transformer oil, v is the average velocity, D_h is the hydraulic diameter and μ is the average dynamic viscosity. It can be seen from the Reynolds numbers obtained from Equation (5.1) that the major forces that affect the flow are the viscous forces.

$$\mathrm{Re} = \frac{\text{inertial forces}}{\text{viscous forces}} = \frac{\rho v D_h}{\mu} \tag{5.1}$$

Dynamic viscosity is defined by molecular viscosity in Fluent software. Average velocity through oil ducts were calculated by using Equation (5.2) that is known as continuity equation, where, A_1 and A_2 are the cross-sectional areas of inlet and oil ducts, also v_1 and v_2 are the velocity of transformer oil at inlet and oil ducts, respectively.

$$A_1 v_1 = A_2 v_2 \tag{5.2}$$

Cross-sectional area at inlet and oil ducts are 282.96 mm^2 and 727.29 mm^2 as shown in Figure 71 and Figure 72, respectively inlet and oil ducts are shown in green in the figures.

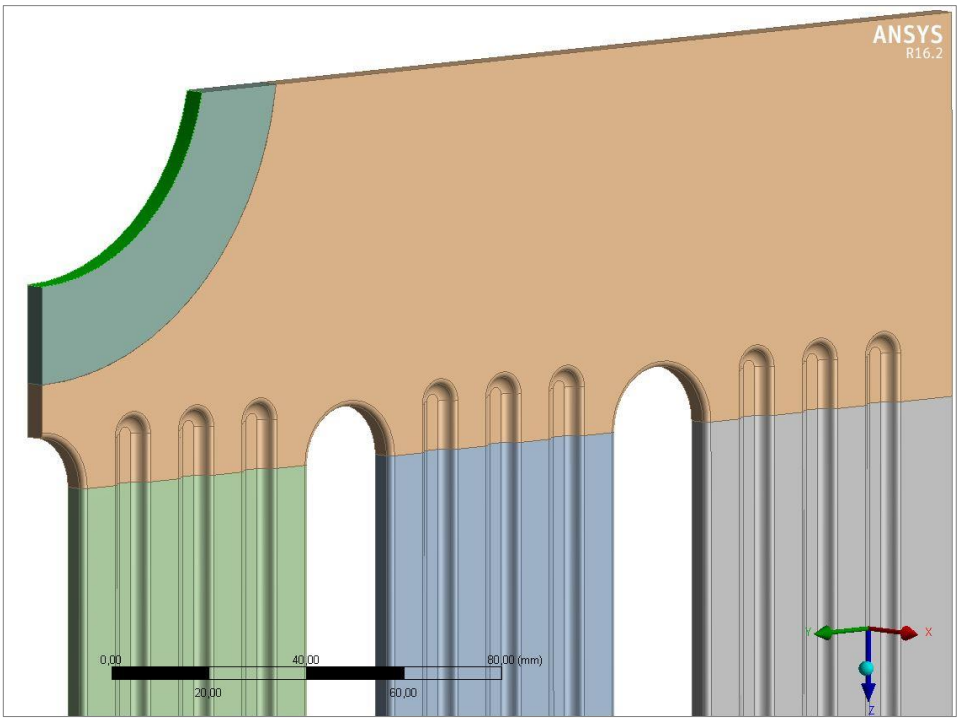

Figure 71. Cross-sectional Area at Inlet.

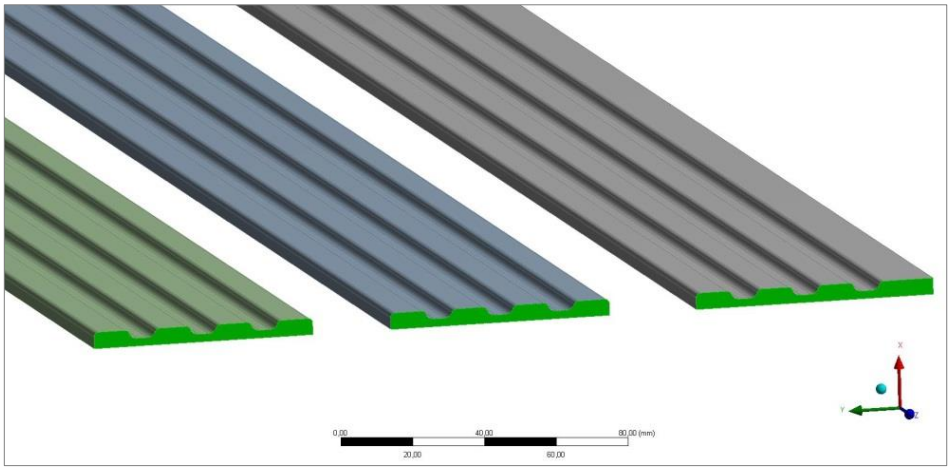

Figure 72. Cross-section Area of Oil Ducts.

Hydraulic diameter is used for non-circular ducts and it is calculated by using Equation (5.3), where, A is the cross-sectional area of oil ducts and P is the wetted perimeter of the cross-section.

$$D_h = \frac{4A}{P} \tag{5.3}$$

Cross-section area of oil ducts and wetted perimeter of the cross-section are shown with green color in Figure 72 and Figure 73, respectively. For this case, cross-sectional area of oil ducts is 727.3 mm^2 and wetted perimeter of the cross-section is 429.5 mm. Then, hydraulic diameter was calculated as shown below by using Equation (5.3).

$$D_h = \frac{4(727.3\ mm^2)}{429.5\ mm}$$

$$D_h = 6.77\ mm.$$

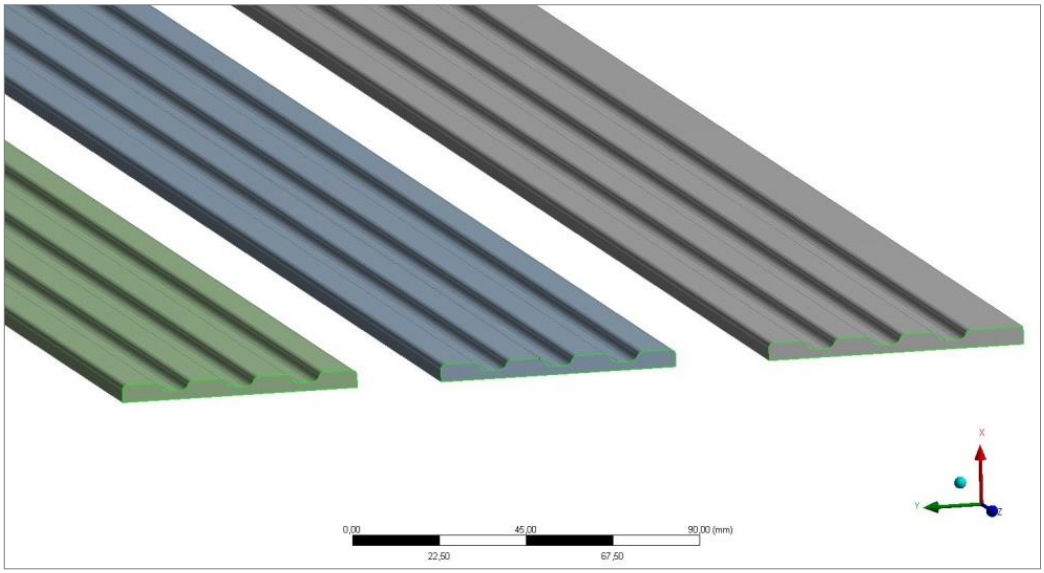

Figure 73. Wetted Perimeter of Oil Duct Cross-section Area.

Calculated Reynolds numbers were very small as shown in Table 11 below. Accordingly, viscous forces directly affect the heat energy dissipation in this study.

Table 11. Reynolds Number of Natural Ester Transformer Oil Flow.

Velocity	**Average Velocity through Oil Ducts**	**Average Density**	**Average Viscosity**	**Reynolds Number**
[*m/s*]	[*m/s*]	[kg/m^3]	[*kg/ms*]	[-]
0.02	0.0078	885.0303	0.0134	3.479
0.03	0.0117	883.4450	0.0127	5.497
0.04	0.0156	882.6011	0.0123	7.560
0.05	0.0195	882.0687	0.0121	9.601

Moreover, calculated Nusselt number and Prandtl number are seen in Table 12 and Table 13, respectively. Nusselt number is a dimensionless number that is the ratio of convective heat transfer to conductive heat transfer as shown in Equation (5.4), where h is the heat transfer coefficient at the film temperature, L is the characteristic length and k is the thermal conductivity of the transformer oil at film temperature. In this study, characteristic length, D_h, was calculated as 6.77 mm. Therefore, theoretical Nusselt number was calculated by using Equation (5.5) as shown in Table 12.

$$Nu = \frac{hL}{k} \tag{5.4}$$

$$Nu = \frac{hD_h}{k} \tag{5.5}$$

Reference values were adjusted in Fluent software so that temperature was given as film temperature and length was given as characteristic length. Film temperature was calculated by using Equation (5.6) to obtain the physical properties. All the related physical properties (density, specific heat, thermal conductivity and viscosity) were evaluated at film temperature as seen in Table 12.

$$T_{film} = \frac{T_{wall} + T_{fluid}}{2} \tag{5.6}$$

Table 12. Theoretical Nusselt Number for Natural Ester Transformer Oil Flow.

Inlet Velocity	**Film Temperature**	**Thermal Conductivity**	**Heat Transfer Coefficient**	**Theoretical Nusselt Number**
[*m/s*]	[*K*]	[*W/m.K*]	[$W/m^2.K$]	[-]
0.02	342.2816	0.1517	111.36	4.97
0.03	344.6465	0.1513	112.77	5.05
0.04	345.9115	0.1510	114.20	5.12
0.05	346.7161	0.1508	115.72	5.20

Furthermore, theoretical Prandtl number was calculated as seen in Table 13. Prandtl number is the ratio of momentum diffusivity to thermal diffusivity as shown in Equation (5.7), where μ is the dynamic viscosity, c_p is the specific heat and k is the thermal conductivity of oil.

$$Pr = \frac{\mu c_p}{k} \tag{5.7}$$

Prandtl number is the main parameter to define relationship between the velocity boundary layer and temperature boundary layer. As shown in calculated Prandtl

numbers in Table 13, viscous diffusion is dominant for transformer oils. Generally, transformer oils have high Prandtl number. Therefore, it can be concluded that the thermal boundary layer of transformer oils is located at the viscous region close to wall.

Table 13. Theoretical Prandtl Number for Natural Ester Transformer Oil Flow.

Inlet Velocity	**Film Temperature**	**Thermal Conductivity**	**Dynamic Viscosity**	**Specific Heat**	**Theoretical Prandtl Number**
[*m/s*]	[*K*]	[*W/m.K*]	[$W/m^2.K$]	[*J/kg.K*]	[-]
0.02	342.2816	0.1517	0.01332	2348.805	206.38
0.03	344.6465	0.1513	0.00127	2354.176	201.25
0.04	345.9115	0.1510	0.01259	2359.159	196.59
0.05	346.7161	0.1508	0.01237	2362.368	193.67

Using the calculated data, a graph between the Nusselt number and Reynolds number was plotted for different velocities. Influence of Reynolds number on Nusselt number was shown in Figure 74. Equation (5.8) shows that the Nusselt number increases linearly as the Reynolds number increases. In Figure 74, blue points indicate the theoretical Nusselt number and the red line obtained by using Equation (5.8).

$$\mathrm{Nu} = 0.0372\ \mathrm{Re} + 4.8419 \tag{5.8}$$

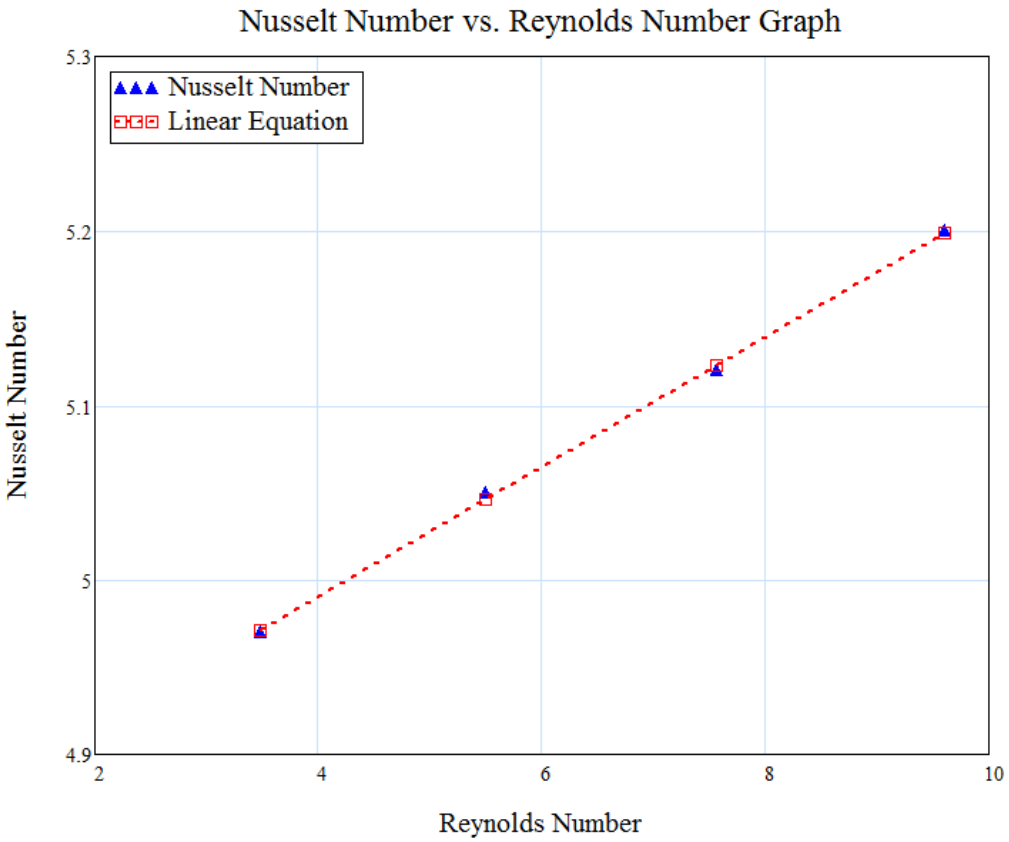

Figure 74. Nusselt Number versus Reynolds Number Graph.

Calculated Nusselt number, Reynolds number and Prandtl number are shown in Table 14 for different velocities.

Table 14. Calculated Dimensionless Numbers at Different Velocities.

Inlet Velocity	**Nusselt Number**	**Reynolds Number**	**Prandtl Number**
[*m/s*]	[-]	[-]	[-]
0.02	4.97	3.479	206.38
0.03	5.05	5.497	201.25
0.04	5.12	7.560	196.59
0.05	5.20	9.601	193.67

The Nusselt number depends on Reynolds number and Prandtl number as shown in Equation (5.9), where a, b and c are constants. Reynolds number is a function of density, velocity, hydraulic diameter and dynamic viscosity as $Re=Re(\rho, v, D_h, \mu)$. Prandtl number is function of dynamic viscosity, specific heat and thermal conductivity as $Pr=Pr(\mu, c_p, k)$.

$$\mathrm{Nu} = \mathrm{C}\,\mathrm{Re}^{\mathrm{a}}\,\mathrm{Pr}^{\mathrm{b}} \tag{5.9}$$

Least-squares method was used to determine the constants a, b and c. Equation (5.9) was separated into two parts to use power law as seen in Equation (5.10) and Equation (5.11), where $\mathrm{C} = \sqrt{\mathrm{C_1 C_2}}$.

$$\mathrm{Nu} = \mathrm{C_1}\mathrm{Re}^{\mathrm{a}} \tag{5.10}$$

$$\mathrm{Nu} = \mathrm{C_2}\mathrm{Pr}^{b} \tag{5.11}$$

Power law was applied to find correlation for Equation (5.10) in MathCAD. The logarithm was taken for both sides of the Equation (5.12) as shown below to use linear regression. Then, u, v and w were defined as u=ln(Nu), v=$\ln(\mathrm{C_1})$ and w=ln(Re). Thus, nonlinear equation was defined as a linear equation as shown in Equation (5.13). The matrix form equation was constituted to find constants a and $\mathrm{C_1}$ as shown in Equation (5.14). Consequently, a and $\mathrm{C_1}$ were obtained as 0.021785 and 4.7, respectively. These steps were applied for the Equation (5.11). Hence, b and $\mathrm{C_2}$ were obtained as 0.68956 and 196.4 respectively.

$$\ln(\mathrm{Nu}) = \ln(\mathrm{C_1}) + \mathrm{a}\ln(\mathrm{Re}) \tag{5.12}$$

$$\mathrm{u} = \mathrm{v} + \mathrm{aw} \tag{5.13}$$

$$\begin{bmatrix} \mathrm{n} & \sum \ln(\mathrm{Re}) \\ \sum \ln(\mathrm{Re}) & \sum \ln(\mathrm{Re})^2 \end{bmatrix} \begin{bmatrix} \ln(\mathrm{C_1}) \\ a \end{bmatrix} = \begin{bmatrix} \sum \ln(\mathrm{Nu}) \\ \sum \ln(\mathrm{Re})\ln(\mathrm{Nu}) \end{bmatrix} \tag{5.14}$$

Equation (5.10) was multiplied by Equation (5.11) then the final correlation was obtained as shown in Equation (5.15).

$$\mathrm{Nu} = 30.41\,\mathrm{Re}^{0.021785}\,\mathrm{Pr}^{-0.344780} \tag{5.15}$$

5.2. Mesh Independence

All analysis studied in this thesis were simulated with 2014258 mesh elements (mesh type – 3) and 0.897 skewness. Mesh independence was also studied with natural transformer oil to validate the results as shown in Table 15.

Table 15. Mesh Independence.

Type	Number of Mesh Elements	Velocity	Outlet Temperature	Pressure Difference	Heat Flux	Skewness
#	[-]	$[m/s]$	$[K]$	$[Pa]$	$[W/m^2]$	[-]
1	8178016	0.05	345.7	190.0	285.9	0.931
2	2143041	0.05	345.7	190.8	284.9	0.899
3	2014258	0.05	345.7	190.8	284.9	0.897
4	1370706	0.05	345.9	191.6	285	0.899

Sweep method was used to generate mesh of oil ducts, inlet zone and outlet zone in all mesh types. Oil ducts were meshed by using sweep bias, which has the biggest element at the middle. Mesh size controls were used on inlet and outlet zones both with (Figure 75) and without bias (Figure 76) in type – 1 and type – 3. Then, skewness was obtained 0.931 and 0.897 for mesh type – 1 and mesh type – 2, respectively. On the other hand, edge sizing controls were not used in mesh type – 4.

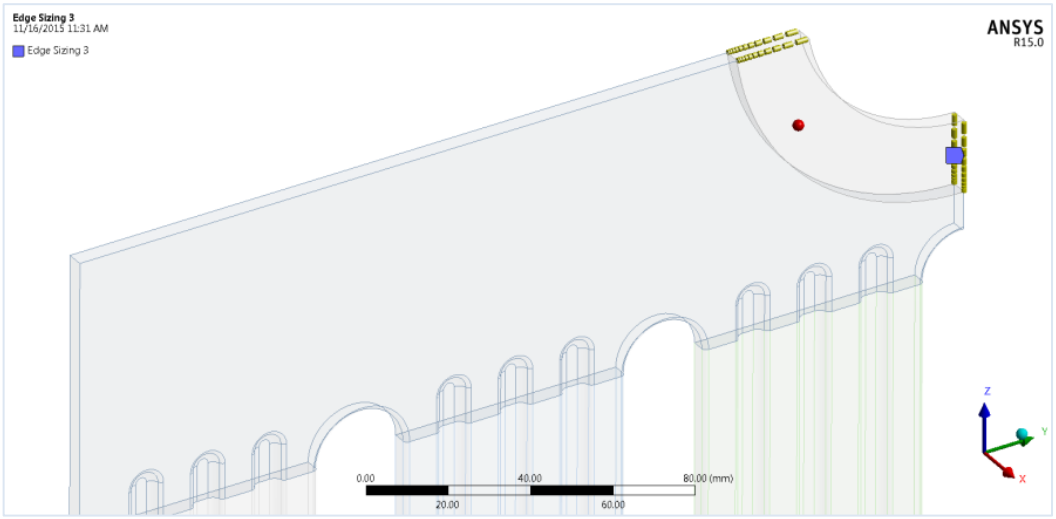

Figure 75. Edge Sizing at Inlet Zone with Bias.

Figure 76. Edge Sizing at Inlet Zone without Bias.

CHAPTER 6

CONCLUSION

This chapter summarizes the thesis, discusses its findings and contributions, shows the limitations, and also presents the future work recommendations.

CFD (Computational Fluid Dynamics) simulation of a power transformer requires significant number of elements. Because of this reason, supercomputers are needed to perform finite volume based simulation programs. At this point, some approaches and assumptions can be useful to simplify problems. Porous media approach is a method to solve complex geometries in Fluent. Flow characteristics and material properties should be known in detail.

Transformer life directly depends on the aging of cellulose based insulation material in winding. The hottest temperature of winding can be determined by using too much element number. For this reason, velocity versus pressure difference graphs can be created to use porous media approach. Then, cooling systems can be defined as porous media in CFD simulations of transformers.

Mineral oils are the most common oil used in oil immersed transformers. However, they have high risk of fire with 170 ˚C. Also, they are not environmentally friendly. On the other hand, natural ester transformer oils are both environmentally friendly and they have 360 ˚C fire point. Natural ester oils are fully biodegradable. They have 97% biodegradability as seen in Table 5. Especially in recent years, environmental issues have become more important at all around the world. Therefore, non-renewable transformer cooling fluids will be replaced with renewable alternative cooling fluids in the near future. Moreover, ester oil and synthetic transformer oils are preferred for wind turbines in Europe and US.

The aim of this study is investigation of transformer radiator and behavior of different types of transformer oil. This study also examines the different types of transformer oil. Radiator model was simulated with using different transformer oils. Outlet temperature, pressure difference, heat flux and temperature difference between inlet and outlet of transformer were presented in Table 7, Table 8, Table 9 and Table 10 with natural ester, mineral, silicone and synthetic transformer oils, respectively. This

study also provides an approach and methodology to researchers, who studies on CFD simulations of transformers. Transformer CFD simulations can be solved by using this methodology.

First step of solution algorithm that is used for transformer hot-spot temperature value was accomplished by this study. Investigation of radiator, oil ducts and cooling system performance will be studied by using this method for cold start works in transformers. Also, improvements to the transformer radiators will be studied. Investigation on radiator groups will be studied to specify the hot-spot locations and cooling performance in the light of this research. Finally, oil flow and heat transfer in winding will be presented in detail. Then, this study will provide a methodology to simulate a transformer in ANSYS Fluent CFD software.

The outcomes of this study will be verified in a special test room. This is a state supported project where the thermal and hydrodynamic performances of transformer cooling systems can be tested in this special test room located in Balikesir Electromechanical Industrial Plants Corporation’s facilities. This test room along with this thesis will provide better understanding of transformer cooling systems.

REFERENCES

Arora, R.K. (2013, December). Different DGA techniques for monitoring of transformers. *International Journal of Electronics and Electrical Engineering, (1),* No.4.

El Wakil, N., Chereches, N.C.&Padet,J. (2006). Numerical study of heat transfer and fluid flow in a power transformer. *International Journal of Thermal Sciences,* 45, 615-626.

Fdhila, R.B., Kranenborg, J., Laneryd, T., Olsson, C., Samuelsson, B., Gustafsson, A.&Lundin, L. (2011). Thermal modelling of power transformer radiators using a porous medium based CFD approach. *Second International Conference on Computational Methods for Thermal Problems,* China.

Fernández, I., Ortiz, A. Delgado, F., Renedo, C.&Pérez,S. (2012). Comparative evaluation of alternative fluids for power transformers. *Electric Power Systems Research, 98,* 58-69.

Fonte, C. M., Lopes, J. C. & Dias, M. M. (2011, 6-9 June). CFD analysis of core type power transformers. *21st International Conference on Electricity Distribution,* Frankfurt.

Gastelurrutia et al. (2009). Numerical modelling of natural convection of oil inside distribution transformers. *Applied Thermal Engineering, (31),* 493-505.

IEC 60076-7 International Standards. Loading guide for oil-immersed power transformers , Part 7, 2005-12.

Joshi, K.U., & Deshmukh, N. K. (2004). Thermal analysis of oil cooled transformer. *Cigre 2004 Session,* Paris, France.

Karsai, K., Kerényi, D.&Kiss, L. (1987). *Large power transformers*. Hungary, Elsevier.

Kim, M., Cho, S.M. & Kim, J.K. (2012). Prediction and evaluation of the cooling performance of radiators used in oil-filled power transformer applications with non-direct and direct-oil-forced flow. *Experimental Thermal and Fluid Science, (44),* 392-397.

Kulkarni, S.V. & Khaparde, S.A. (2005). *Transformer engineering design and practice*. India, Mercel Dekker Inc.

Radakovic, Z. & Sorgic, M. (2010). Basics of detailed thermal-hydraulic model for thermal design of oil power transformers. *IEEE Transactions on Power Delivery, 25*(2), 790-802.

Rozga, P. (2013). Properties of new environmentally friendly biodegradable insulating fluids for power transformers. *1st Annual International Interdisciplinary Conference, AIIC 2013,* 24-26 April, Portugal.

Skillen, A., Revell, A., Iacovides, H.&Wu, W. (2011). Numerical prediction of local hot-spot phenomena in transformer windings. *Applied Thermal Engineering, 36,* 96-105.

Southern Nevada Regional Professional Development Program. (n.d.).Physical science. Retrieved October 3, 2015 from the World Wide Web: *http://www.rpdp.net/sciencetips_v2/P12C6.htm*

Wittmaack, R. (2014). Thermal design of power transformers via CFD. *11th. World Congress on Computational Mechanics (WCCM XI).*